Journal of Sound and Vibration (1999) **227**(1), 29–64
Article No. jsvi.1999.2327, available online at http://www.idealibrary.com on IDEAL®

THE RESPONSE OF A SWEPT BLADE ROW TO A THREE-DIMENSIONAL GUST

S. A. L. Glegg

Center for Acoustics and Vibration, Florida Atlantic University, Boca Raton, FL 33431, *U.S.A.*

(*Received* 25 *June* 1998, *and in final form* 9 *April* 1999)

An analytical expression is obtained for the unsteady loading, acoustic mode amplitude, and sound power output of a three-dimensional rectilinear cascade of blades with finite chord excited by a three dimensional gust. The effects of spanwise wave number and cross-flow are included so that the effect of blade sweep and a gust with a spanwise variation can be considered. The results show that the effect of the spanwise gust and blade sweep are very similar and reduce the effective frequency of the incoming gust. The dominant effect is caused by the cut off of acoustic modes when the trace velocity of the gust along the blade span is subsonic.

1. INTRODUCTION

The unsteady aerodynamics and aeroacoustics of ducted fans are an important aspect of aeroengine design. For example, it is currently believed that the primary source of fan tone noise is the result of the interaction between the rotor blade wakes and downstream stator vanes. To address this problem, the response of a set of uniformly spaced blades to an incoming vortical gust needs to be considered. Many different approaches have been used for this calculation but, as will be discussed below, none give a complex analytical solution for a skewed gust incident on a set of blades whose edge may be swept relative to the mean flow direction.

In the 1970s, several studies were carried out on two-dimensional sets of blades which were represented by a cascade of flat plates at zero angle of attack [1–6]. Kaji and Okazaki [1] considered sound propagation upstream through a cascade by solving for a distribution of dipole sources on the blade surfaces. In this approach, the solution of the integral equation which relates the source strength to the velocity disturbance was obtained using a collocation procedure. In a subsequent paper, Kaji and Okazaki [2] used the same approach to evaluate the sound generated by a rotor wake/stator interaction. Mani and Hovray [3] also considered the sound transmission problem but used an approximate solution based on the Wiener Hopf method. Although they gave an analytical result they assumed that there was no interaction between the leading and trailing edges of the blades. Koch [4] extended the Wiener Hopf analysis of Mani and Hovray [3] to

0022-460X/99/410029 + 36 $30.00/0

blades with finite chord and gave the transmission and reflection coefficient for both upstream and downstream propagating acoustic waves.

Koch's method provides the analytical basis for the solution to the cascade problem, but numerical solutions which are based on a similar approach to that of Kaji and Okazaki [1] have proven to be more versatile [5, 6]. For example, Smith [6] developed a code which gives the unsteady loading, the vortical field, and the acoustic field upstream or downstream of a two-dimensional blade row for any type of incoming gust. In recent years, these types of analyses have been extended to loaded cascades with finite thickness blades using numerical solutions to the Euler equations (see references [7, 8] for reviews). All the methods are accurate and computationally efficient at low reduced frequencies but at high reduced frequencies, when the gust wavelength is short compared to the blade chord these methods are computationally time-consuming.

The recent development of very high by-pass aeroengines, which have blades with much larger blade chords than in previous designs, has led to renewed interest in analytical methods for the blade response function at high frequencies. Analytical methods are important in this application because they can provide high-frequency asymptotic solutions. In this regard, Peake [9] has extended Koch's [4] analysis to give the unsteady loading on the blades caused by an incoming vortical gust, and has also developed analytical tools [10, 11] which enable rapid evaluation the functions required for the Wiener Hopf solution [3, 4].

All the studies described above only consider two-dimensional cascades and a more accurate model of an aeroengine is given by a rotor and/or a stator in a circular duct. As a first approximation, Atassi and Hamad [12] considered the three-dimensional rectilinear cascade model described by Goldstein [13], subject to a rotor wake or secondary flow disturbance. The unsteady loading and sound generation by a ducted rotor was considered by Namba [14]. The solution is obtained by solving an integral equation for the velocity potential using a collocation method and numerical results showed that three-dimensional effects reduced the blade loading at low frequencies and non-zero spanwise wavenumbers reduced the acoustic radiation at high frequencies. Kordama and Namba [15] extended this analysis to a rotor with swept blades and Schulten [16] introduced a alternative form for the Greens function in a circular duct to evaluate the acoustic radiation from swept stator vanes downstream of a fan. See also recent work by Chiang [17] and Golubev *et al.* [18].

The objective of this paper is to consider the acoustics of swept blade rows by evaluating the response function for a three-dimensional incoming gust. An analytical solution will be sought by considering a rectilinear cascade of flat plates at zero angle of attack in a uniform cross-flow (see Figure 1). The two-dimensional models discussed above cannot be used for this problem because they do not include the effect of the spanwise unsteady loading which dominates the ultimate response. The only previous analytical study on this model is the approximate analysis of Envia and Kerschen [19]. They considered a three-dimensional rectilinear cascade of finite span with the leading edge of the blades swept back in the downstream direction. To simplify the analysis they assumed blades with semi-infinite chord and neglected coupling between the blades. The response

function of each blade was assumed to be the same as the response of an isolated airfoil of semi-infinite extent. Consequently, they did not include any of the blade gap effects which are important features of the two-dimensional cascade models. This paper will reconsider the model proposed by Envia and Kerschen [19] and include both the effect of finite chord blades and the blade coupling. The results given below are an exact analytical solution to the cascade problem and include all the features of the model given by Koch [4] for the two-dimensional case.

This study considers blades which have finite chord and are subject to either an incoming vortical or acoustic disturbance as shown in Figure 1. In section 2, we will set up the basic equations for this flow and specify the boundary conditions which must be satisfied. In section 3, the solution to these equations will be given in terms of the pressure distribution on the blade surfaces. The analysis is based on the Wiener Hopf method and is laid out in Appendix A. In section 4, we will consider the unsteady blade loading as a function of reduced frequency, spanwise wavenumber and blade sweep angle. In section 5, expressions will be given for the sound power for each radiating mode and results will be shown which demonstrate the effect of blade sweep on the acoustic radiation.

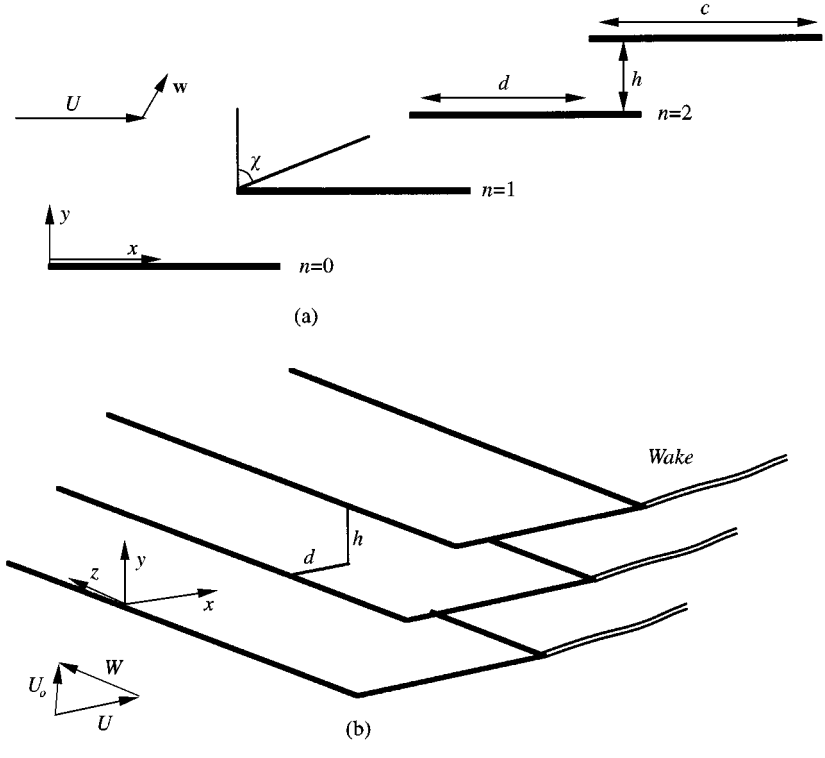

Figure 1. A linear cascade of blades in a uniform flow (a) side view showing an incident velocity perturbation given by **w**. (b) three dimensional view showing spanwise mean flow velocity W and blade wakes.

2. THE EQUATIONS OF MOTION AND BOUNDARY CONDITIONS FOR A WAVE INCIDENT ON A CASCADE

Consider a linear cascade of fan blades in a uniform subsonic flow, as illustrated in Figure 1. It will be assumed that there is either a vortical or acoustic wave incident on the cascade which causes a velocity perturbation $\mathbf{w}$ to the mean flow. The cascade consists of a set of infinitely thin flat plates of chord c which have a stagger angle χ. The cascade is defined in three dimensions (x, y, z) with mean flow parallel to the blade surfaces with velocity components (U, O, W). The flow normal to the blade surfaces will be zero and so the incident velocity perturbation $\mathbf{w}$ will induce a scattered field which must satisfy the linear equations of fluid motion. If the velocity perturbation of the scattered field is $\mathbf{u}$ then the boundary condition on the surface of each blade will be $(\mathbf{w} + \mathbf{u})\cdot\mathbf{n} = 0$ where $\mathbf{n}$ is normal to the surface. In addition, the blade will shed vorticity into its wake which is convected downstream by the steady flow. The wake cannot support a discontinuity in pressure and this imposes a Kutta condition at the trailing edge of each blade.

It is convenient to solve this problem using the velocity potential for the scattered field which is defined by $\nabla\phi = \mathbf{u}$. The momentum equation then relates the pressure and the velocity potential as $p_s = -\rho_0 \mathrm{D}\phi/\mathrm{D}t$ and the continuity equation becomes

$$\frac{1}{c_0^2}\frac{\mathrm{D}^2\phi}{\mathrm{D}t^2} - \nabla\phi = 0. \tag{1}$$

We will seek a solution to this equation using integral transforms which will require taking an integral of all the terms in equation (1). However, there is a fundamental difficulty in this approach because the velocity field, and hence ϕ, has discontinuity across each blade and its wake. Consequently, the derivatives of ϕ are not integrable functions. To correctly allow for this we specify the jump in the potential across the blades and the wakes as $\Delta\phi_n$ and introduce generalized derivatives, such that

$$\frac{1}{c_0^2}\frac{\mathrm{D}^2\phi}{\mathrm{D}t^2} - \tilde{\nabla}^2\phi = -\frac{\partial}{\partial y}\sum_n \Delta\phi_n(x, z, t)\delta(y - nh) - \sum_n \Delta\left[\frac{\partial\phi_n(x, z, t)}{\delta y}\right]_n \delta(y - nh), \tag{2}$$

where the first term on the left accounts for the discontinuity in velocity potential across the blades and the wakes, and the second term allows for a discontinuity in the velocity normal to the blades and the wakes. Because the incident gust is continuous everywhere and the blades are infinitesimally thin, the boundary condition on the surface of the blades ensures that there is no jump in the flow velocity normal to the blade. However, this would not be the case if the blades had finite thickness. Furthermore, the wake cannot be a source of mass injection and so the velocity normal to the wake surface must be continuous across the wake. These conditions assure that the last term in equation (2) is zero.

The incident gust is assumed to be a harmonic wave with an upwash velocity field given by

$$\mathbf{w}\cdot\mathbf{n} = w_0 e^{-i\omega' t + i\gamma_0 x + i\alpha y + ivz}. \tag{3}$$

If follows that the scattered field will also have a time dependence of $\exp(-i\omega' t)$ and that the upwash encountered on each blade and wake will be shifted in phase by $\sigma = \gamma_0 d + \alpha h$ (see Figure 1). This phase shift is one of the controlling features of the cascade response and is referred to as the interblade phase angle. The gust described by equation (3) is perfectly general and can be used to represent a vortical gust which is convected downstream or an acoustic wave propagating either upstream or downstream.

Since each blade encounters an upwash with the same amplitude, it follows that the response of each blade will have the same magnitude relative to the leading edge, but will be shifted in phase by the interblade phase angle. Consequently, we can write

$$\Delta\phi_n(x, z, t) = \Delta\phi_0(x - nd) e^{-i\omega' t + in\sigma + ivz}, \tag{4}$$

where $\Delta\phi_0(x) = 0$, $x < 0$. Substituting this into equation (2) we obtain

$$\frac{1}{c_0^2}\frac{D^2\phi}{Dt^2} - \tilde{\nabla}^2\phi = -\frac{\partial}{\partial y}\sum_n \Delta\phi_0(x - nd)\delta(y - nh) e^{-i\omega' t + in\sigma + ivz}. \tag{5}$$

A solution to this equation can be obtained using the method of integral transforms. First, we note that since the blades have infinite span the scattered field will be harmonic in time and can be defined as

$$\phi(\mathbf{x}, t) = \phi(x, y) e^{-i\omega' t + ivz}. \tag{6}$$

Then we define the Fourier integral transform and its inverse in the (x, y) plane as

$$f(\gamma, \mu) = \frac{1}{(2\pi)^2}\int_{-\infty}^{\infty}\int_{-\infty}^{\infty} F(x, y) e^{i\gamma x + i\mu y}\, dx\, dy, \quad F(x, y) = \int_{-\infty}^{\infty}\int_{-\infty}^{\infty} f(\gamma, \mu) e^{-i\gamma x - i\mu y}\, d\gamma\, d\mu \tag{7}$$

Applying this transform to equation (5) gives

$$(-(\omega' + \gamma U - vW)^2/c_0^2 + \gamma^2 + \mu^2 + v^2)\phi(\gamma, \mu) = \frac{i\mu}{2\pi}\sum_n D(\gamma) e^{in(\sigma + \gamma d + \mu h)} \tag{8}$$

where $D(\gamma)$ is the Fourier transform of $\Delta\phi_0(x)$ and is defined as

$$D(\gamma) = \frac{1}{2\pi}\int_0^{\infty} \Delta\phi_0(x) e^{i\gamma x}\, dx. \tag{9}$$

At this point we will specify $\omega = \omega' - vW$, then taking the inverse of equation (8) gives

$$\phi(x, y) = \frac{1}{2\pi}\int_{-\infty}^{\infty}\int_{-\infty}^{\infty} \frac{-\mathrm{i}\mu D(\gamma)}{(\omega + \gamma U)^2/c_0^2 - \gamma^2 - \mu^2 - v^2}\left\{\sum_n \mathrm{e}^{\mathrm{i}n(\sigma + \gamma d + \mu h)}\right\}\mathrm{e}^{-\mathrm{i}\gamma x - \mathrm{i}\mu y}\,\mathrm{d}\gamma\,\mathrm{d}\mu. \tag{10}$$

Note how the velocity potential of the scattered field is specified by the function D which is the Fourier transform of the discontinuity across the blades and the wakes. To obtain D, equation (10) must be combined with the boundary conditions to give an integral equation which can be solved by using the Wiener Hopf method.

The integral over μ in equation (10) can be carried out using the residue theorem by requiring that the wave field decays at large distances from the blade where it originates. This moves the poles of the integrand in the complex μ plane either below or above the real axis and the integral is calculated from the residue at the poles to give

$$\phi(x, y) = \frac{1}{2}\int_{-\infty}^{\infty} D(\gamma)\left\{\sum_n \mathrm{sgn}(nh - y)\mathrm{e}^{\mathrm{i}n(\sigma + \gamma d) + \mathrm{i}\zeta|nh - y|}\right\}\mathrm{e}^{-\mathrm{i}\gamma x}\,\mathrm{d}\gamma, \tag{11}$$

$$\zeta = \sqrt{(\omega + \gamma U)^2/c_0^2 - \gamma^2 - v^2},$$

where $\mathrm{Im}(\zeta) > 0$. This result will be used to match the boundary conditions on the surface of the blade which is specified in terms of the velocity normal to the surface as

$$\frac{\partial\phi(x, 0)}{\partial y} = 2\pi\int_{-\infty}^{\infty} D(\gamma)j(\gamma)\mathrm{e}^{-\mathrm{i}\gamma x}\,\mathrm{d}\gamma, \tag{12}$$

where we have taken $y = 0^+$ and defined

$$j(\gamma) = \frac{\mathrm{i}\zeta}{4\pi}\left\{\sum_{n=-\infty}^{\infty} \mathrm{e}^{\mathrm{i}n(\sigma + \gamma d) + \mathrm{i}\zeta|nh|}\right\}. \tag{13}$$

The right-hand side of equation (12) is in the form of an inverse Fourier transform which may be written as a convolution integral in the form

$$\frac{\partial\phi(x, 0)}{\partial y} = \int_0^{\infty} \Delta\phi_0(x_0)K(x - x_0)\,\mathrm{d}x_0, \tag{14}$$

where $K(x)$ is given by the inverse Fourier transform of equation (13). To obtain the solution for $\Delta\phi_0$ or D we will solve equation (14) subject to the boundary conditions of

(1) zero normal velocity to the blade surface,

$$\partial\phi(x, 0)/\partial y + w_0 e^{i\gamma_0 x} = 0, \quad 0 < x < c; \tag{15}$$

(2) zero pressure jump across the blade wake,

$$\frac{D(\Delta\phi_0(x)e^{-i\omega' t + ivz})}{Dt} = 0, \quad x > c; \tag{16}$$

(3) no discontinuities upstream of the leading edge,

$$\Delta\phi_0(x) = 0, \quad x < 0. \tag{17}$$

The problem is completely specified by equation (12)–(17) and various methods are available for solving these equations. In the next section, we will show how this may be achieved using the Wiener Hopf method.

3. SOLUTION TO THE INTEGRAL EQUATION

3.1. SPECIFICATION OF THE BOUNDARY VALUE PROBLEM

The Wiener Hopf method may be used to solve integral equations of the type given by equation (14) subject to the boundary conditions given by equations (15) and (17) in the limit that c tends to infinity. However, in the case of interest here the boundary conditions are specified over a finite chord and so a modified method is required to obtain a solution. To achieve this, we solve the problem in four parts by defining the unknown $\Delta\phi_0$ or D as the sum of four different solutions:

$$\Delta\phi_0 = \Delta\phi_0^{(1)} + \Delta\phi_0^{(2)} + \Delta\phi_0^{(3)} + \Delta\phi_0^{(4)} \tag{18}$$

and

$$D = D^{(1)} + D^{(2)} + D^{(3)} + D^{(4)},$$

where each solution satisfies the integral equation

$$f^{(i)}(x) = \int_0^\infty \dot{\Delta}\phi_0^{(i)}(x_0) K(x - x_0)\, dx_0. \tag{19}$$

To obtain the complete solution we first obtain a solution to equation (19) subject to the boundary conditions

$$f^{(1)}(x) = \frac{\partial \phi}{\partial y} = -w_0 e^{i\gamma_0 x}, \quad x > 0; \qquad \Delta\phi_0^{(1)}(x) = 0, \quad x < 0. \tag{20}$$

The solution for $i = 1$ therefore ensures that the velocity normal to the blade and its wake is zero. To satisfy the Kutta condition given by equation (16), we solve equation (19) with $i = 2$, subject to the boundary conditions

$$f^{(2)}(x) = 0, \quad x < c; \quad \frac{D(\Delta\phi_0^{(1)}(x)e^{-i\omega' t + ivz} + \Delta\phi_0^{(2)}(x)e^{-i\omega' t + ivz})}{Dt} = 0 \quad x > c. \tag{21}$$

However the solution for $\Delta\phi_0^{(2)}$ does not satisfy the boundary condition given by equation (17) and so we must introduce two additional solutions which are coupled and satisfy equation (19) with the boundary conditions

$$f^{(3)}(x) = 0, \quad x > 0; \quad \Delta\phi_0^{(2)}(x) + \Delta\phi_0^{(3)}(x) + \Delta\phi_0^{(4)}(x) = 0, \quad x > 0; \tag{22}$$

and

$$f^{(4)}(x) = 0, \quad x < c; \quad \frac{D(\Delta\phi_0^{(3)}(x)e^{-i\omega' t + ivz} + \Delta\phi_0^{(4)}(x)e^{-i\omega' t + ivz})}{Dt} = 0, \quad x > c. \tag{23}$$

The boundary value problems defined by equations (20)–(23) are all defined on a semi-infinite part of the x-axis, and so are suitable for solution using the Wiener Hopf method. At the same time the sum of the solutions satisfy the boundary conditions given by equations (15)–(17). Consequently, the cascade response can be obtained from four boundary value problems defined on semi-infinite parts of the x-axis, for which there is a known method of solution. Each of these boundary value problems is solved in Appendix A giving the complete solution for $D(\gamma)$.

3.2. THE DISCONTINUITY OF VELOCITY POTENTIAL

Adding the solutions for each of the boundary value problems defined above gives the Fourier transform of the discontinuity in velocity potential as

$$D(\gamma) = \left\{ \frac{-iw_0}{(2\pi)^2(\gamma + \gamma_0)J_+(\gamma)J_-(-\gamma_0)} \right\} - \left\{ \sum_{n=0}^{\infty} \frac{(A_n + C_n)e^{i(\gamma - \delta_n)c}}{i(\omega + \gamma U)(\gamma - \delta_n)} \left[\frac{J_-(\delta_n)}{J_-(\gamma)} \right] \right\} - \left\{ \sum_{m=1}^{\infty} \frac{B_m}{(\gamma - \varepsilon_m)} \left[\frac{J_+(\varepsilon_m)}{J_+(\gamma)} \right] \right\}. \tag{24}$$

The result is the sum of the three terms in $\{\ \}$ and each of these has a specific physical interpretation. The first term is the response of a set of semi-infinite chord blades to an incident gust. The second term is the correction required to allow the wake to satisfy the Kutta condition and the third term ensures that there are no discontinuities introduced upstream of the leading edge of the blade. The coefficients A_n and C_n represent the contributions from the first and second order wake corrections defined by the boundary value problems given by equations (21) and (23) respectively. The functions $J_+(\gamma)$ and $J_-(\gamma)$ are defined by equation (A.18) and are generated from the splitting of the function $j(\gamma)$ which is required for the application of the Wiener Hopf method. The function $J_+(\gamma)$ has no singularities or zeros in the upper half of the complex γ plane, but in the lower half plane $J_+(\gamma)$ has zeros at $\gamma = \delta_n = \kappa M + \theta_{n-1}$ (see equation (A.15)) and an infinite number of simple poles at $\gamma = \kappa M + \eta_n^-$ (see equation (A.17)). Similarly, $J_-(\gamma)$ has no singularities or zeros in the lower half of the complex γ plane, but in the upper half plane $J_-(\gamma)$ has zeros at $\gamma = \varepsilon_n = \kappa M + \vartheta_{n-1}$ and an infinite number of simple poles at $\gamma = \kappa M + \eta_n^+$. The coefficients A_n, B_n, C_n are defined in equations (A.26), (A.50) and (A.47) respectively.

Each term in equation (24) has singularities in the complex plane but the sum of all the terms ensures that $D(\gamma)$ is analytic everywhere in the complex plane apart from at $\gamma = -\omega/U$ (see sections A.3 and A.4). This provides some insight into the effects which contribute to the discontinuity in potential and the pressure discontinuity on the blade surfaces. To obtain $\Delta\phi(x)$ we evaluate the inverse Fourier transform of equation (24) defined as

$$\Delta\phi(x) = \int_{-\infty - i\tau_1}^{\infty - i\tau_1} D(\gamma) e - i\gamma x \, d\gamma. \tag{25}$$

This integral may be evaluated by using the residue theorem and closing the contour in either the upper or the lower part of the complex plane. The choice of contour depends on the convergence of the integrand at large γ and this can be considered in three separate regions. First when $x < 0$ the contour must be closed in the upper half plane where $D(\gamma)$ has no singularities and so the value of the integral is zero. Second, in the region $x > c$ the contour must be closed in the lower half plane where $D(\gamma)$ has a single pole at $\gamma = -\omega/U$ which occurs in the second term of equation (24). This singularity gives a solution for the integral which has a wave convected at the mean flow speed in the wake and represents a vortical disturbance which is required to satisfy the Kutta condition. However, this discontinuity in potential does not cause any pressure discontinuity across the wake and so does not radiate any acoustic waves. Finally, we must consider the value of the integral when $0 < x < c$ which gives the potential discontinuity on the surface of the blade. The term J_+ and J_- have algebraic growth at large values of γ and so the choice of contour will depend on the arguments of the exponential in the integrand when equation (24) is inserted in equation (25). The first and the last terms of equation (24) will cause a dependence of the form $\exp(-i\gamma x)$ and so the contour should be closed in the lower half plane for these terms. In contrast, the

second term in equation (24) has a dependence of $\exp(-\mathrm{i}\gamma(x-c))$ and so these terms must be evaluated using a contour in the upper half plane when $x < c$. The important point here is that the cancellation of the singularities which applies when all the terms of equation (24) are added together, no longer occurs, and so the poles of each individual term in both the upper and lower half plane will contribute to the integral. The complete solution is then given as

$$\Delta\phi(x) = 2\pi\mathrm{i}\sum_{n=0}^{\infty}\frac{A_n \mathrm{e}^{-\mathrm{i}\delta_n x}}{\mathrm{i}(\omega+\delta_n U)} + \left\{\sum_{n=0}^{\infty}\sum_{m=1}^{\infty}\frac{(A_n+C_n)\,\mathrm{e}^{\mathrm{i}\varepsilon_m(c-x)-\mathrm{i}\delta_n c}}{\mathrm{i}(\omega+\varepsilon_m U)(\varepsilon_m-\delta_n)}\left[\frac{J_-(\delta_n)}{J'_-(\varepsilon_m)}\right]\right\}$$
$$+\left\{\sum_{n=0}^{\infty}\sum_{m=1}^{\infty}\frac{B_m \mathrm{e}^{-\mathrm{i}\delta_n x}}{(\delta_n-\varepsilon_m)}\left[\frac{J_+(\varepsilon_m)}{J'_+(\delta_n)}\right]\right\}, \quad 0 < x < c. \tag{26}$$

4. THE UNSTEADY LOADING

4.1. THE UNSTEADY LOADING AND NUMERICAL ACCURACY

The results given in the previous section also allow the unsteady loading on the blade to be evaluated. The unsteady loading is defined as the integral of the unsteady pressure over the blade surface is customarily non-dimensionalized as the coefficient $C_p = L/\pi\rho_0 U_0 w_0 c$ where L is the unsteady loading per unit span and $U_0 = (U^2 + W^2)^{1/2}$. To obtain this we evaluate

$$C_p = \frac{1}{\pi\rho_0 U_0 w_0 c_0}\int_0^c -\rho_0\frac{\mathrm{D}\Delta\phi}{\mathrm{D}t}\,\mathrm{d}x \tag{27}$$

and by comparison with equation (9) we obtain

$$C_p = \frac{2\mathrm{i}\omega D(0)}{U_0 w_0 c}, \tag{28}$$

where $D(0)$ can be obtained from equation (24), and $\Delta\phi(0) = 0$. (This follows from asymptotic evaluation of equation (24) when $\gamma \sim \infty$).

To verify that the approach described here agrees with calculations using other methods, a series of tests have been carried out and the results compared with published computations. For example, Atassi [7] gives calculations which show the unsteady loading as a function of $\gamma_0 c$ for an incoming two-dimensional vortical wave ($\gamma_0 = \omega/U$) with no cross-flow ($W = 0$) with $\alpha = \gamma_0$, $M = 0{\cdot}3$, $\chi = 40^\circ$ and $s/c = 0{\cdot}6$. The results obtained using the method described here are shown in Figure 2 and are in agreement with Atassi's calculations over the frequency range $0 < \gamma_0 c < 20$. To eiminate any numerical singularities in the evaluation of equation (24), $D(0)$ in equation (28) is replaced by $D(\mathrm{i}\varepsilon)$ with $\varepsilon = 10^{-3}$. The series calculations for $J_\pm(\gamma)$ are evaluated using 1000 terms and the matrices needed for the calculation of the leading and trailing edge corrections (see section A4) include at least three non-propagating modes and a minimum of seven modes in total.

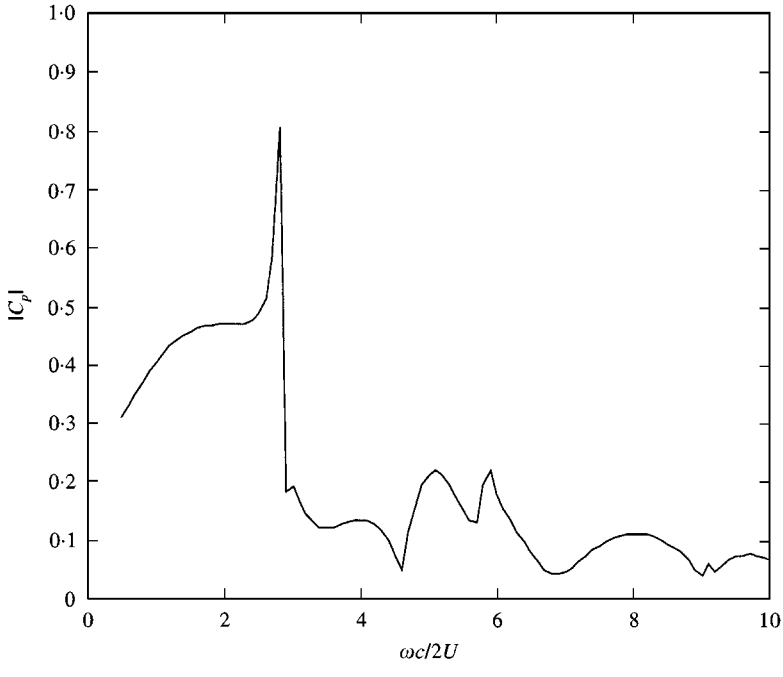

Figure 2. Example of the unsteady lift response of a flat-plate cascade for the case given by Atassi [7].

Additional tests using the Smith code [6, 20] have shown that numerical agreement is obtained up to the third decimal place for typical calculations.

4.2. CHARACTERISTICS OF THE UNSTEADY LIFT RESPONSE FUNCTION

The unsteady loading is obtained from equations (28) and (24) as

$$C_p = \frac{2\mathrm{i}\omega}{U_0 w_0 c}\left[\left\{\frac{-\mathrm{i}w_0}{(2\pi)^2\gamma_0 J_+(0)J_-(-\gamma_0)}\right\} + \left\{\sum_{n=0}^{\infty}\frac{(A_n + C_n)\mathrm{e}^{-\mathrm{i}\delta_n c}}{\mathrm{i}\omega\delta_n}\left[\frac{J_-(\delta_n)}{J_-(0)}\right]\right\} + \left\{\sum_{m=1}^{\infty}\frac{B_m}{\varepsilon_m}\left[\frac{J_+(\varepsilon_m)}{J_+(0)}\right]\right\}\right]. \tag{29}$$

The first term in $\{\ \}$ represents the contribution from the blades in the absence of the trailing edge. It is the result which would be obtained from blades with semi-infinite chord. The second term represents the correction for the trailing edge. The last term represents the correction to ensure the boundary conditions are satisfied upstream of the leading edge after the trailing edge correction is applied. Therefore, it represents an additional leading edge contribution which is a consequence of waves generated at the trailing edge travelling upstream and being scattered at the leading edge.

To illustrate the general features of this function, Figure 3 shows the magnitude of the unsteady lift as a function of the non-dimensional wavenumber for a case similar to that given by Atassi [7] ($M = 0{\cdot}3$, $\chi = 40^\circ$, $s/c = 0{\cdot}6$) but with a constant interblade phase angle of $\sigma = 3\pi/4$. The results identify two important regions where the unsteady lift has an increased magnitude. At $\omega c/2U = 4$ there is a large peak and at $\omega c/2U = 7$ there is a minimum. It will be shown in the next section that the acoustic modes which propagate away from the cascade cut on when $\kappa_e = \pm f_m$ in equation (A.17). The minimum in the blade response occurs exactly at the cut on frequency.

The high levels in the blade response at $\omega c/2U \approx 12$ are associated with the high order modes in the blade passages. The chordwise wavenumber for these modes is given by

$$\delta_n = \kappa M - \sqrt{\kappa_e^2 - \left(\frac{(n-1)\pi}{\beta h}\right)^2}, \quad \varepsilon_m = \kappa M + \sqrt{\kappa_e^2 - \left(\frac{(m-1)\pi}{\beta h}\right)^2},$$

$$\kappa = \omega/c_0\beta^2, \quad \beta^2 = 1 - M^2, \quad \kappa_e^2 = \kappa^2 - (\nu/\beta)^2 \tag{30}$$

and so the first higher order blade passage mode ($n, m = 2$) cuts on when $\kappa_e = \pm \pi/\beta h$ which corresponds to $\omega c/2U = 10{\cdot}86$.

It is interesting to consider the unsteady lift response if only the first order terms of equation (29) are included, as was done in reference [10]. This can lead to significant errors in the estimation of the blade response function, especially around the cut-on frequencies of the modes. To illustrate this, Figure 4 compares calculations obtained using only the semi-infinite blade and the first order trailing

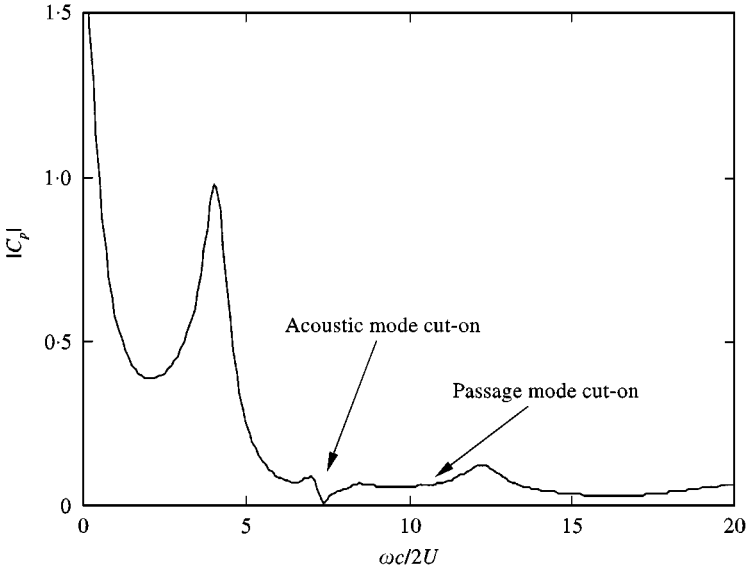

Figure 3. Example of the unsteady lift repsonse of a flat plate cascade.

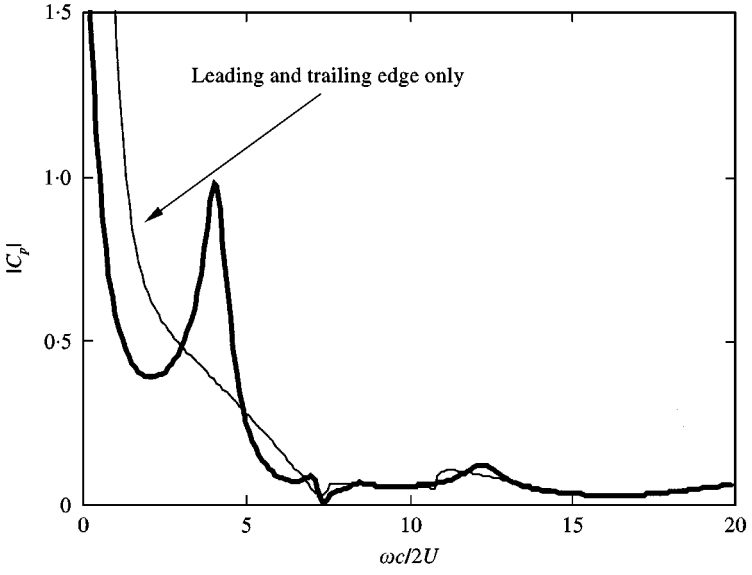

Figure 4. Comparison between the complete and approximate solutions: —, approximate solution using leading and travelling-edge terms only; ——, complete solution.

edge correction (given by the terms A_n) with the complete response (given by equation (29)). Above the acoustic mode cut on frequency the two methods give very similar results, but below the cut on there are large differences. The wave field which is trapped in the blade passages is therefore very important to the overall response of the system at low frequencies.

The results given above are for a two-dimensional cascade but can easily be extended to include the effect of a spanwise gust. To illustrate the effect of the spanwise wavenumber, Figure 5 shows the unsteady lift at a fixed non-dimensional frequency $\omega c/2U = 10$ as a function of vc. The effect of the spanwise wavenumber is to reduce the value of $\kappa_e = (\kappa^2 - v^2/\beta^2)^{1/2}$ while κ and γ_0 remain constant. In this example the acoustic mode is cut on when the spanwise wavenumber is zero. However as the spanwise wavenumber is increased there is a corresponding reduction in κ_e and when $\kappa_e < f_m$ the acoustic mode is cut off. The acoustic mode cuts off for all spanwise wave numbers in excess of $vc = \beta(\kappa^2 - f_m^2)^{1/2}c$ which in this example is 3·82. At the cut on frequency there is a minimum in the unsteady lift followed by a rapid rise and a peak. This characteristic is the same as expected at frequencies just below cut on for the two-dimensional case shown in Figure 3, indicating that the primary effect of the spanwise wavenumber is to cause mode to cut off and this is associated with a peak in the unsteady lift.

4.3. THE EFFECT OF BLADE SWEEP

One of the advantages of this approach is that the effect of blade sweep can be introduced directly. To achieve this the leading edges of the blades are rotated so

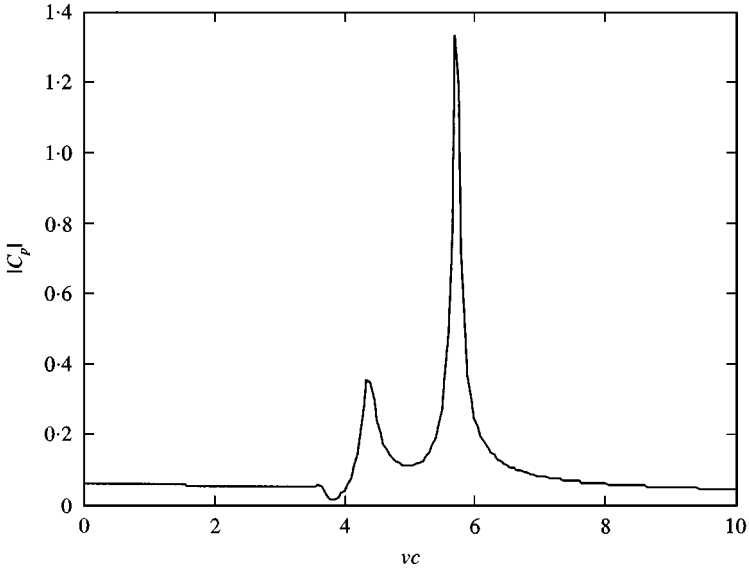

Figure 5. Example of the unsteady lift response of a flat-plate cascade as a function of spanwise wavenumber.

they make an angle φ with the flow (see Figure 6). The leading edge of the blades will then be located at

$$x = nd_0 \cos\varphi, \quad y = nh,$$

where φ is the angle of sweep (see Figure 6). If the mean flow speed is U_0 then the effect of sweep is to reduce the inflow velocity in the direction of the blade chord such that $U = U_0 \cos(\varphi)$, and cause a spanwise flow $W = U_0 \sin(\varphi)$. For an incoming vortical gust the incoming wavenumbers in the chordwise and the spanwise direction will also be changed so that $\gamma_0 = (\omega'/U_0)\cos(\varphi)$ and $v = (\omega'/U_0)\sin(\varphi)$. If d_0 is independent of sweep this translation causes the blade spacing in the chordwise direction to be reduced to $d = d_0 \cos\varphi$ and this has the effect of reducing the interblade phase angle to $\sigma = (\omega' d/U_0)\cos^2(\varphi) + \alpha h$ and the inflow angle to $\chi = \tan^{-1}(d_0 \cos(\varphi)/h)$. Also, in deriving equation (10) an effective frequency was introduced which was defined as $\omega = \omega' - vW = \omega' \cos^2(\varphi)$. The effect of sweep is therefore to reduce the effective inflow velocity, interblade phase angle and to introduce a spanwise wavenumber.

Figure 7 shows the unsteady lift as a function of sweep angle for the same conditions which were used in the examples given above with d_0 constant. The result are very similar to the results for a spanwise gust indicating that the effect of sweep on the spanwise wavenumber of the gust dominates the response rather than changes in the effective flow speed or interblade phase angle. The acoustic mode cuts off when the sweep angle is $\sim 11{\cdot}5^\circ$ and at higher angles of sweep the unsteady lift shows a large peak as expected just below the cut-off frequency. In conclusion the primary effect of sweeping the blades is to cut off the acoustic modes generated by the cascade because of the increased spanwise wavenumber component.

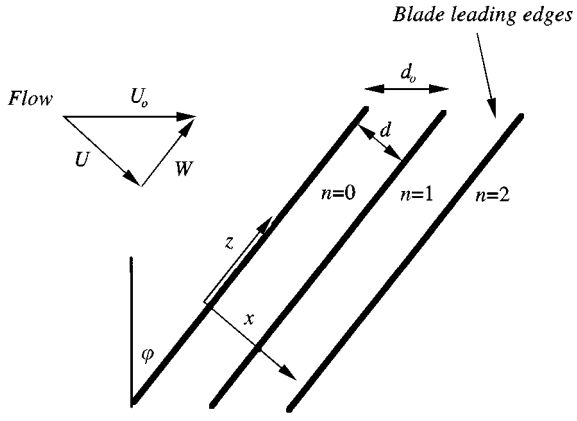

Figure 6. The rotated co-ordinates for a swept blade row.

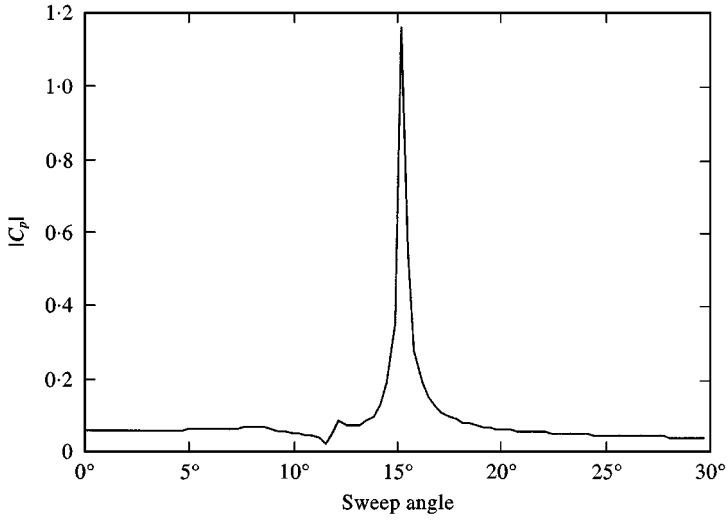

Figure 7. The effect of blade sweep on the unsteady lift response of a flat-plate cascade

5. THE ACOUSTIC MODES

5.1. THE ACOUSTIC FIELD

The acoustic radiation from the cascade can be obtained from the evaluation of the integral given in equation (11). The integrand includes a summation which may be evaluated in the same manner as was used for the evaluation of equation (13) (see section A.2) and gives, for $0 < y < h$,

$$\phi(x, y) = \frac{-1}{2} \int_{-\infty}^{\infty} D(\gamma) \left\{ \frac{e^{i(\zeta h - \gamma d)\, y/h}}{1 - e^{i\zeta h - i\gamma d - i\sigma}} + \frac{e^{-i(\zeta h + \gamma d)\, y/h}}{1 - e^{-i\zeta h - i\gamma d - i\sigma}} \right\} e^{-i\gamma(x - yd/h)}\, d\gamma. \quad (31)$$

To make use of the residue theorem the integral is completed on a contour at infinity and providing that $y < h$ the exponential terms in $\{\ \}$ will tend to zero on this contour. The contour should be closed in the lower half plane when $x - yd/h > 0$ which is downstream of the blades, and in the upper half plane when $x - yd/h < 0$ which is upstream of the blades. We have already shown that the function $D(\gamma)$ has an isolated singularity in the complex plane at $\gamma = \gamma_0$. It is relatively easy to show that this results in a convected (non-propagating) wave which decays exponentially with distance from each blade wake. The only contributions to the acoustic field will come from the singularities of the terms in $\{\}$. The integrand has a branch cut along $\zeta = 0$, but since it is an even function of ζ, the contribution from the branch cut will be zero. There are however contributions from the singularities which occur when $\zeta h \pm (\gamma d + \sigma) = \pm 2\pi n$. These singularities occur at the same locations as the singularities for the function $j(\gamma)$. Using equation (A.17) and evaluating the residue at the poles of the integrand then gives

$$\phi(x, y) = \pi \sum_{m=-\infty}^{\infty} \zeta_m^{\pm} D(\lambda_m^{\pm}) \left\{ \frac{e^{i(\sigma - 2\pi m)y/h}}{\eta_m^{\pm} h\beta^2 \pm \zeta_m^{\pm} d} \right\} e^{-i\lambda_m^{\pm}(x - yd/h)},$$

$$\lambda_m^{\pm} = \kappa M + \eta_m^{\pm}, \quad \zeta_m^{\pm} = \beta(\kappa_e^2 - (\eta_m^{\pm})^2)^{1/2}, \tag{32}$$

where the upper sign is used in the upstream direction and the lower sign is used in the downstream direction, and $\eta_m^{\pm}$ is defined in equation (A.17).

This result enables us to identify how the amplitude of each propagating mode depends on the function $D(\gamma)$. In the region upstream of the cascade this function is evaluated at the locations in the upper half plane where $j(\gamma)$ and hence $J_-(\gamma)$ has singularities. Consideration of equation (24) shows that, at these locations, the trailing edge correction term is identically zero and so for upstream radiation we need only consider

$$D(\lambda_m^+) = \frac{-iw_0}{(2\pi)^2(\lambda_m^+ + \gamma_0)J_+(\lambda_m^+)J_-(-\gamma_0)} - \left\{ \sum_{n=0}^{\infty} \frac{B_n}{(\lambda_m^+ - \varepsilon_n)} \left[\frac{J_+(\varepsilon_n)}{J_+(\lambda_m^+)} \right] \right\}. \tag{33}$$

Similarly in the region downstream of the cascade only the trailing edge terms are non-zero, hence for downstream radiation we need only consider

$$D(\lambda_m^-) = -\left\{ \sum_{n=0}^{\infty} \frac{(A_n + C_n)e^{i(\lambda_m^- - \delta_n)c}}{i(\omega + \lambda_m^- U)(\lambda_m^- - \delta_n)} \left[\frac{J_-(\delta_n)}{J_-(\lambda_m^-)} \right] \right\}. \tag{34}$$

This shows how the upstream radiation is determined by the leading-edge contributions while the downstream radiation is determined by the trailing-edge corrections. This split will be discussed in more detail in the next section.

5.2. THE SOUND POWER OUTPUT

The sound power output of the cascade is obtained by integrating the acoustic intensity of the field over a surface which encloses all the sources. In the model

defined in section 2, the blades have infinite span and the cascade has an infinite number of blades. This represents a circular fan with a finite number of blades B and span b. To allow for the periodicity of the actual fan the incoming disturbance and the radiated field will repeat after B blade gaps and the surface enclosing the sources should be drawn as illustrated in Figure 8. The sound power W is then obtained from the integral

$$W = \int_S \mathbf{I} \cdot \mathbf{n} \, \mathrm{d}S, \tag{35}$$

where $\mathbf{n}$ is the outward drawn normal to the surface and the acoustic intensity is defined for harmonic sources [13] as

$$\mathbf{I} = \frac{1}{2} \mathrm{Re} \left\{ \left(\frac{p}{\rho_0} + \mathbf{U} \cdot \mathbf{u} \right) (\rho_0 \mathbf{u} + \rho' \mathbf{U})^* \right\}. \tag{36}$$

This may be written in terms of the velocity potential by using $p = -\rho_0 \mathrm{D}\phi/\mathrm{D}t$ and $\rho' = p/c_0^2$ so that

$$\mathbf{I} = \frac{-\rho_0}{2} \mathrm{Re} \left\{ \frac{\partial \phi}{\partial t} \left(\nabla \phi - \frac{\mathbf{U}}{c_0^2} \frac{\mathrm{D}\phi}{\mathrm{D}t} \right)^* \right\}. \tag{37}$$

To evaluate the sound power the acoustic intensity must be evaluated on the surface shown in Figure 8. This includes the upper and lower surfaces A_+ and A_- but since the cascade is an upwrapped version of a fan with B blades the field will be identical on these two surfaces and so they will not contribute to the sound power. Similarly for the surfaces which enclose the sources in the spanwise direction; equation (37) shows that the acoustic intensity is independent of spanwise location and so the contribution of the spanwise end caps will be zero. The sound power can then be defined in terms of the integrals over the upstream or downstream surfaces

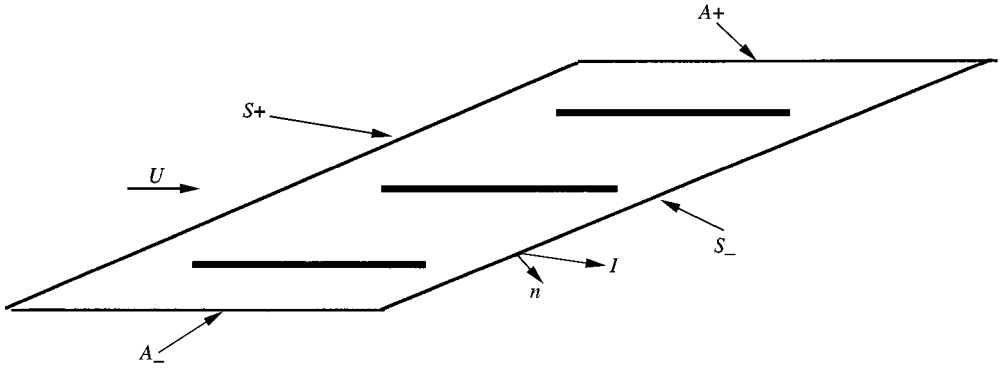

Figure 8. The surfaces enclosing the blades which are used for the evaluation of the sound power.

S_+ or S_-. The contribution from each is defined as the upstream or downstream sound power, respectively, and can be evaluated by considering the acoustic intensity upstream or downstream of the cascade. This is obtained by using equation (32) which gives

$$\mathbf{I} = \frac{\omega' \rho_0 \pi^2}{2} \mathrm{Re} \sum_{m,n} \left\{ \frac{\zeta_m^{\pm} D(\lambda_m^{\pm})}{\eta_m^{\pm} h\beta^2 \pm \zeta_m^{\pm} d} \right\} \left\{ \frac{\zeta_n^{\pm} D(\lambda_n^{\pm})}{\eta_n^{\pm} h\beta^2 \pm \zeta_n^{\pm} d} \right\}^* \times [\lambda_n^{\pm} \hat{\mathbf{x}} - (\lambda_n^{\pm} d + \sigma - 2\pi n)\hat{\mathbf{y}}/h - v\hat{\mathbf{z}} - \mathbf{U}(\omega + U\lambda_n^{\pm})/c_0^2]^* \times \mathrm{e}^{2\pi \mathrm{i}(n-m)y/h - \mathrm{i}(\lambda_m^{\pm} - \lambda_n^{\pm})(x - yd/h)}. \tag{38}$$

The surfaces S_+ and S_- are defined along lines where $x - yd/h = const$ and y lies in the range $0 < y < Bh$. The surface integral therefore ensures that only those terms for which $m = n$ yield non-zero values of sound power and so all the cross-terms in equation (38) are eliminated. The normal to the surface is defined as $\mathbf{n} = \pm(-h/s, d/s, 0)$, where $s = (d^2 + h^2)^{1/2}$ is the blade spacing. We then obtain the upstream or downstream sound power as

$$W_{\pm} = \frac{\omega' \rho_0 Bb\pi^2}{2} \mathrm{Re} \sum_m \frac{|\zeta_m^{\pm} D(\lambda_m^{\pm})|^2}{\zeta_m^{\pm} d \pm \eta_m^{\pm} h\beta^2}. \tag{39}$$

The denominator in this equation can be simplified by making use of the definitions given in equation (A.17) giving a preferable form of this result as

$$W_{\pm} = \frac{\omega' \rho_0 Bb\pi^2}{2\beta s e} \mathrm{Re} \sum_m \frac{|\zeta_m^{\pm} D(\lambda_m^{\pm})|^2}{\sqrt{\kappa_e^2 - f_m^2}},$$

$$s_e = \sqrt{d^2 + (h\beta)^2}, \quad f_m = (\sigma + \kappa M d - 2\pi m)/s_e. \tag{40}$$

This result shows that sound power is only generated when the modes are cut on ($\kappa_e > f_m$) and is inversely proportional to the blade spacing. At the cut-on frequency ($\kappa_e = f_m$) there is a singularity but consideration of $D(\lambda_m^{\pm})$ shows that the sound power goes zero at cut-on. This is apparent because $D(\lambda_m^{\pm})$ is inversely proportional to $J_{\pm}(\lambda_m^{\pm})$ and the limiting behavior of $J_{\pm}(\lambda_m^{\pm})$ close to the cut-on frequency of the mth mode is determined by the product terms in the denominator of equation (A.18) for which

$$\left(1 - \frac{\eta_m^{\pm}}{\eta_m^{\mp}}\right)^{-1} = \frac{\mp \eta_m^{\mp}}{2 \cos \chi_e (\kappa_e^2 - f_m^2)^{1/2}}.$$

Using this relationship in the expression for the sound power, equation (40), shows that the sound power tends to zero at cut on in proportion to $(\kappa_e^2 - f_m^2)^{1/2}$. To avoid numerical singularities a small imaginary part $\varepsilon\kappa M$ is added to $(\kappa_e^2 - f_m^2)^{1/2}$ in the definition of $\lambda_m^{\pm}$ and in the denominator of equation (40).

5.3. THE CHARACTERISTICS OF THE MODAL SOUND POWER

Figure 9 shows the downstream sound power (normalized by $\rho_0 w_0^2 U_0 Bbs/2$) for each propagating mode as a function of frequency for the same parameters as used in the previous examples ($M = 0{\cdot}3$, $\chi = 40^\circ$, $s/c = 0{\cdot}6$, $\sigma = 3\pi/4$). The first mode ($m = 0$) cuts on at a frequency of $\omega c/2U = 7{\cdot}62$. At frequencies just above the cut on there is a large peak in the sound power output followed by a decay to zero at the frequency where $\zeta_m = 0$. Physically, this corresponds to the wavenumber for which the mode propagates downstream in the direction of the flow, in line with the blade chord. The acoustic dipoles on the blade surface generate no power in this direction. At higher frequencies, the sound power increases again for the first mode and it is the dominant contributor at frequencies where $\omega c/2U \approx 25$. The second mode ($M = 1$) cuts on at $\omega c/2U = 8{\cdot}5$ but does not radiate strongly until $\omega c/2U = 12{\cdot}5$. In contrast with the first mode, there is no zero power propagation direction at the lower frequencies because the propagation angle is downwards ($\sigma - 2\pi m < 0$) and so is never aligned with the flow direction (see Figure 1).

To illustrate the importance of the coupling between the leading and trailing edges, Figure 10 shows the comparisons between the exact power output for the first mode and the approximate solution obtained by using the first order trailing-edge solution only, specified by putting $C_n = 0$ in equation (34). The approximate solution overpredicts the power output close to the cut-on frequency (see Figure 10) and at high frequencies the exact solution includes an oscillation which is not present in the approximate solution. A similar feature is also found for

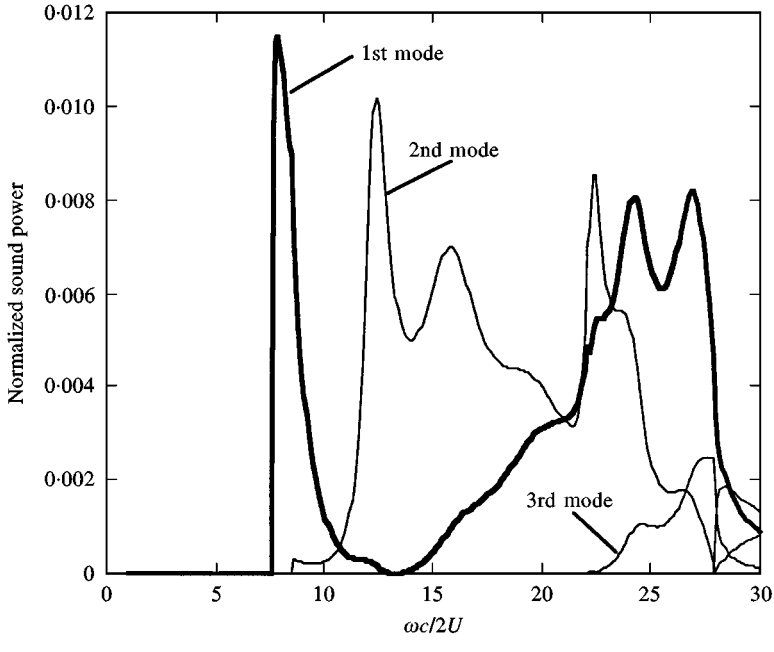

Figure 9. Sound power output for each mode in the downstream direction.

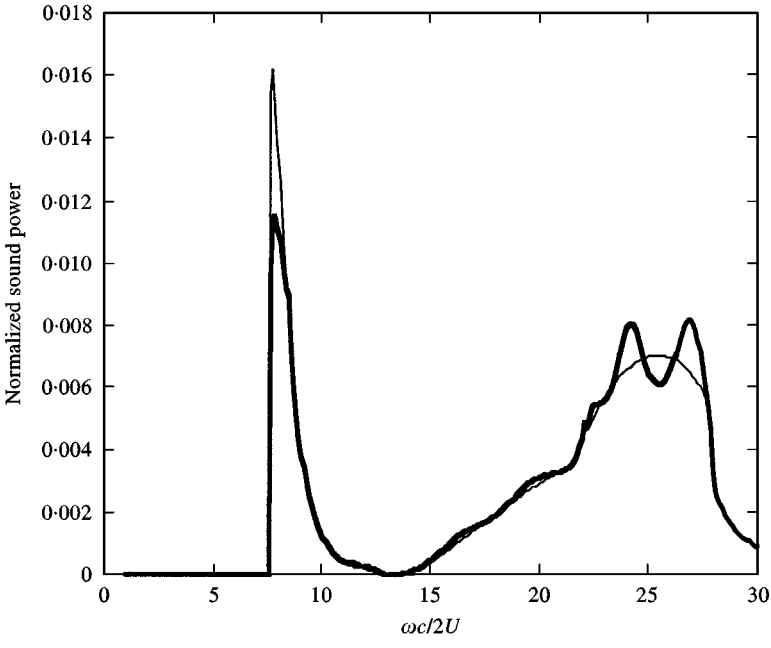

Figure 10. Comparison of approximate (—) and exact solution (——) for the sound power output in the downstream direction for the first mode.

the second mode (Figure 11), especially in the oscillatory region of the curve, and it can be concluded that there is significant interaction between the leading and trailing edges caused by blade passage modes. This has the largest effect on the sound power output when the power is a maximum. Interestingly, the approximation works well when the power output is a minimum.

To illustrate the effect of a three-dimensional gust, Figure 12 shows the sound power of each mode at the frequency $\omega c/2U = 15$ as a function of the spanwise wavenumber. Comparison with Figure 9 shows that at this frequency the second mode dominates. As the spanwise wavenumber is increased the value of κ_e is reduced and this effectively reduces the propagation wavenumber in the direction of the flow. The features of the curves in Figure 12 are therefore similar to the features of the curves in Figure 9, but in reverse, up to the cut-off frequency where $\kappa_e = (\kappa^2 - (v/\beta)^2)^{1/2} = |f_m|$. Notice how the radiated power level is transferred from one mode to another as the first mode cuts off.

One of the interesting features of this result is the fact that the first mode cuts off at a lower spanwise wavenumber than the second mode, whereas at zero spanwise wavenumber the first mode cuts on at a lower frequency. The cut-on characteristics can be understood more easily by considering the wavenumbers which determine the cut-on characteristics. Figure 13 shows the variation of $|f_m c|$ and $\kappa_e c$ as a function of $\omega c/2U$ for the parameters used in this example. The modes are cut on when $\kappa_e = (\kappa^2 - (v/\beta)^2)^{1/2} > |f_m|$, and so the cut-on frequencies can be determined from this graph by the intersections of the curves marked f_m with the curves marked κ for zero spanwise wavenumber and κ_e for the spanwise wavenumber of $vc = 8$.

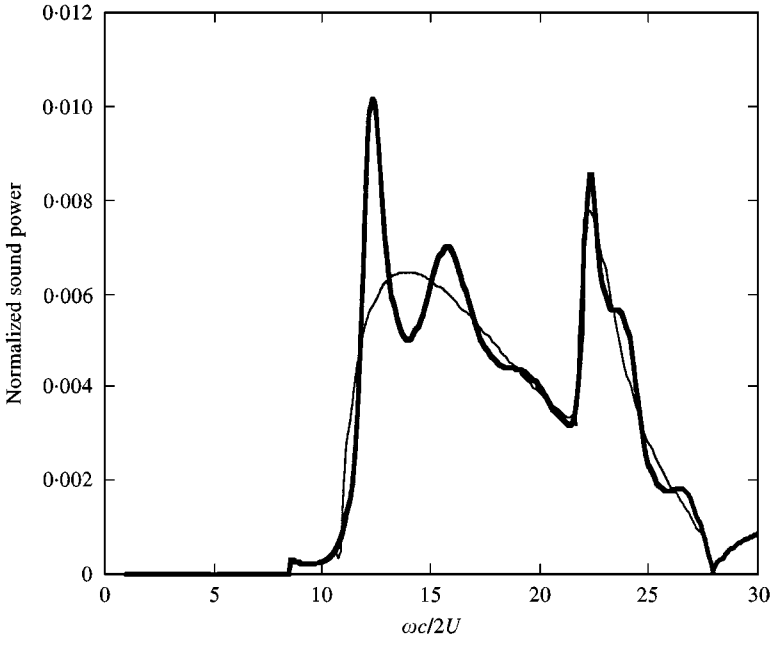

Figure 11. Comparison of approximate (—) and exact solution (▬) for the sound power output in the downstream direction for the second mode.

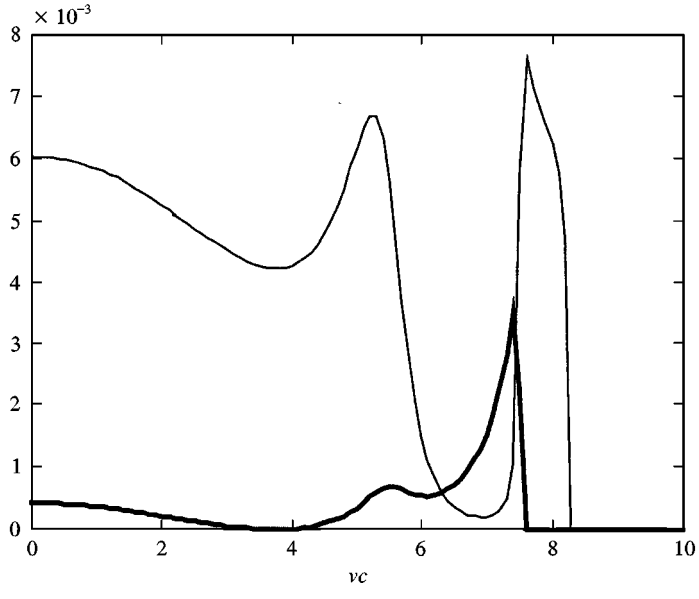

Figure 12. Sound power output in the downstream direction for the first (▬) and second (—) mode as a function of spanwise wavenumber for a non-dimensional frequency of $\omega c/2U = 15$.

The cut-on frequency for the first mode ($m = 0$) occurs at a lower frequency than for the second and third modes ($m = 1, 2$) for the zero spanwise wavenumber, but for $\nu c = 8$ the second mode cuts on before the first mode. The curve for κ_e moves to the right for increased values of νc and this explains why the first mode cuts off before

the second mode Figure 12. This characteristics is a feature of modes with finite spanwise wavenumber and is not apparent from a two-dimentional model. The cross-over point of the curves for $|f_0|$ and $|f_1|$ is determined by their values at zero frequency and the dependence of f_m on κMd. At zero frequency f_m depends on the interblade phase angle (see equation (40)). In the example shown in Figure 13, $\sigma = 3\pi/4$, and when $\sigma \sim 0$ the cross-over point moves to higher frequency. However when $\sigma \sim \pi$ the second mode ($m = 1$) always cuts on at a lower frequency than the first mode ($m = 0$) providing that the Mach number is not zero.

To investigate the effect of blade sweep the same approach is used as in section 4.3 by allowing the cross-flow velocity to be non-zero while reducing the inflow velocity so that $U_0 = (U^2 + W^2)^{1/2}$ remains constant. The effect of increasing the sweep angle is shown in Figure 14 for the high-frequency case $\omega c/2U = 15$. As with the unsteady loading it is seen that the effect of sweep is essentially the same as the effect of increasing the spanwise wavenumber. The primary advantage of using blade sweep is to cause the propagating modes to become cut off. In this case, 15° of sweep is sufficient to achieve cut off for both modes. A simple expression can be derived for the sweep angle required to achieve cut off for a particular mode, φ_m, which is given as

$$\tan \varphi_m = \frac{M}{\beta}\sqrt{1 - f_m^2/\kappa^2}. \tag{41}$$

Consequently, large amounts of sweep are required to achieve cut off for high Mach number flows, but the sweep angle required to achieve cut off of all the modes is not excessive. Also note that the trace velocity of the gust in the spanwise direction is $U_T = U \cot \varphi$ and so for a mode to propagate we require $U_T = U \cot \varphi > U \cot \varphi_m = \beta c_0/(1 - f_m^2/\kappa^2)^{1/2} > \beta c_0$. Consequently, the trace velocity of the gust in the

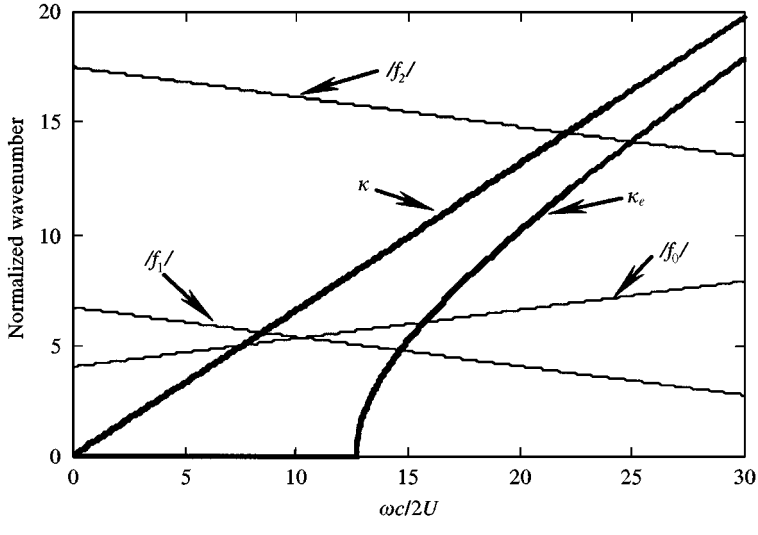

Figure 13. The wavenumbers which determine the cut on frequencies, normalized by blade chord for the parameters defined in the text and a spanwise wavenumber $vc = 8$.

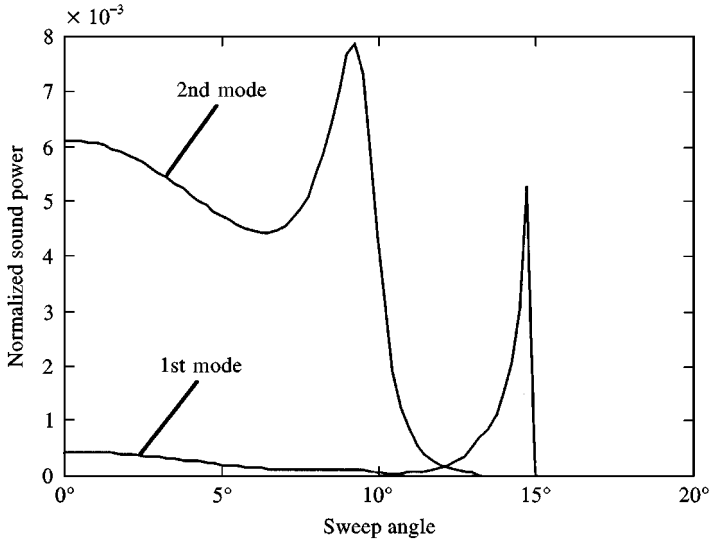

Figure 14. Sound power output in the downstream direction for the first and second modes as a function of sweep angle for a non-dimensional frequency of $\omega c/2U = 15$.

spanwise direction across the leading edge of the blade should be supersonic for mode propagation to occur.

The analysis presented here only applies to subsonic flows for which $U < c_0$ which ensures that $\beta^2 > 0$. For supersonic flows the analysis given in Appendix A needs to be significantly modified. However, an interesting case occurs when the blade is swept in a supersonic flow such that $U_0 > c_0$ but $U < c_0$ so the analysis given here still applies.

The analysis given above for blade sweep does not include the effect of the spanwise wavenumber or blade lean. However, the results of this study show that the primary effect of sweep is to introduce a spanwise wavenumber which causes the propagating modes to be cut off. Similar effects can be expected when the gust is skewed or blade lean is introduced and dispersion curves, such as those given in Figure 13, can be developed for these more complicated cases to identify the frequency ranges where the modes are cut off.

6. CONCLUSIONS

A method has been developed to compute the response of a cascade to a three-dimensional incoming acoustic or vortical wave. The method is based on the Wiener Hopf method but is not limited to low or high frequencies. However, the calculation of the function $J_{\pm}$ which require the evaluation of an infinite series is time-consuming at high frequencies. Peake [10, 11] has suggested several methods for speeding up these calculations but these methods have not been used here.

An expression is given for the unsteady blade loading and this is found to be a strong function of the spanwise wavenumber and/or blade sweep. These parameters reduce the effective frequency of the gust causing the loading response

to be very similar to a lower frequency gust with the same interblade phase angle. Sweep also reduces the flow velocity normal to the leading edge of the blade but this appears to be of secondary importance. It was also found that the unsteady loading at low frequencies is very dependent on the coupling between the leading and trailing edges of the blades and if all the terms required for the complete solution are not included then significant errors occur.

Expressions are also given for the power output of each acoustic mode. This can be described by a leading edge contribution upstream of the blade row and a trailing edge contribution downstream of the blade row. However, the interaction of the leading and trailing edges can never be ignored because the errors in this approximation are worst when the power output is a maximum.

The primary effect of blade sweep on the radiated sound power is to cause the propagating acoustic modes to become cut off. The amount of sweep required to achieve cut off of all modes is proportional to the flow Mach number and requires the trace velocity of the gust along the blade leading edge to be subsonic. Since the primary effect of sweep is to alter the spanwise phasing of the gust, its effect on blade row design can be evaluated relatively easily.

ACKNOWLEDGMENT

This work was supported by NASA grant number NAG 1-1202. The author would also like to thank Donald B. Hanson of Pratt and Whitney and Ray Chi of UTRC for valuable discussions and for pointing out the features of the unsteady lift as a function of spanwise wavenumber.

REFERENCES

1. S. Kaji and Okazaki 1970 *Journal of Sound and Vibration* **11**, 355–375. Propagation of sound waves through a blade row II: analysis based on the acceleration potential method.
2. S. Kaji and Okazaki 1970 *Journal of Sound and Vibration* **13**, 281–307. Generation of sound by a rotor stator interaction.
3. R. Mani and G. Hovray 1970 *Journal of Sound and Vibration* **12**, 59–83. Sound transmission through blade rows.
4. W. Koch 1971 *Journal of Sound and Vibration* **18**, 111–128. On transmission of sound through a blade row.
5. S. Fleeter 1973 *AIAA Journal* **10**, 93–98. Fluctuating lift and moment coefficients for cascaded airfoils in a non-uniform compressible flow.
6. S. N. Smith 1973 *Aeronautical Council R&M* 3709. Discrete frequency sound generation in axial flow machines.
7. H. M. Atassi 1994 *Aerodynamics and Aeroacoustics*, (K-Y. Fung, Editor) Singapore: World Scientific. Unsteady aerodynamics of vortical flows: early and recent developments.
8. J. M. Verdon 1993 *AIAA Journal* **31**, 235–250. Review of unsteady aerodynamic methods for turbomachinery aeroelastic and aeroacoustic applications.
9. N. Peake 1993 *Wave Motion* **18**, 255–271. The scattering of vorticity waves by an infinite cascade of flat plates in subsonic flow.
10. N. Peake 1992 *Journal of Fluid Mechanics*, **241**, 261–289. The interaction between a high frequency gust and a blade row.

11. N. Peake and E. J. Kerschen 1995 *Proceedings of the Royal Society* **449**, 177–186. Uniform asymptotic approximation for high frequency unsteady cascade flow.
12. H. Atassi and G. Hamad 1981 *AIAA paper no.* 81-2046, *presented at the 7th AIAA Aeroacoustics Conference.* Sound generated in a cascade by three dimensional disturbances convected in a subsonic flow.
13. M. E. Goldstein 1976 *Aerocaustics.* New York: McGraw-Hill.
14. M. Namba 1977 *Journal of Sound and Vibration* **50**, 479–508. Three dimensional analysis of blade force and sound generation for an annular cascade in distorted flows.
15. H. Kordama and Namba 1989 *ASME paper no.* 89-GT-306. Unsteady lifting surface theory for a rotating cascade of swept blades.
16. J. B. H. M. Schulten 1997 *AIAA Journal* **35**, 945–951. Vane sweep effects on rotor/stator interaction noise.
17. H-W. D. Chiang and S. Fleeter 1990 *Noice Control Engineering Journal.* Cascade aeroacoustics including steady loading effects.
18. V. V. Golubev, A. I. Lipatov and H. M. Atassi 1997 *AIAA paper* 97–634. 3D unsteady effects in annular cascades with swirl and comparison with 2D strip theory.
19. E. Envia and E. J. Kerschen 1986 *AIAA paper no.* 86-1872, *presented at the 10th Aeroacoustics Conference, Seattle, Washington.* Noise generated by convected gusts interacting with swept airfoil cascades.
20. R. Chi 1996 *Private Communication.*
21. P. M. Morse and H. Feshbach 1953 *Methods of Theoretical Physics.* New York: McGraw-Hill

APPENDIX A: THE WIENER HOPF ANALYSIS

This Appendix describes the solution to the problem defined in section 3.1. The solution is in four parts as defined in equation (18).

A.1. THE CASCADE WITH SEMI-INFINITE CHORD

First we will solve the problem specified by the boundary condition given by equation (20) which is equivalent to considering the response of a cascade with blades which extend to infinity in the downstream direction. To obtain the solution we first take the Fourier transform of equation (19) which can be written as

$$F_{-}^{(1)}(\gamma) + F_{+}^{(1)}(\gamma) = 2\pi D^{(1)}(\gamma) j(\gamma), \tag{A.1}$$

where we have defined of the left-hand side using the Fourier transforms

$$F_{+}^{(1)}(\gamma) = \frac{1}{2\pi}\int_{0}^{\infty} f^{(1)}(x)\mathrm{e}^{\mathrm{i}\gamma x}\,\mathrm{d}x, \quad F_{-}^{(1)}(\gamma) = \frac{1}{2\pi}\int_{-\infty}^{0} f^{(1)}(x)\mathrm{e}^{\mathrm{i}\gamma x}\,\mathrm{d}x, \tag{A.2}$$

so that the boundary condition (20) can be used to specify $F_{+}^{(1)}$ but both $D^{(1)}$ and $F^{(1)}$ are unknowns. To obtain a solution for $D^{(1)}$ from equation (A.1) we need to eliminate $F_{-}^{(1)}$, and to achieve this we will make use of the properties of equation (A.2) in the complex γ plane. We must be careful in this regard because the integrals defining the Fourier transforms may not converge for all values of γ. For

example, if $f^{(1)}(x)$ has exponential decay given by $\exp(-\tau_1 x)$ as x tends to large positive values, then the integral for $F_+^{(1)}$ converges when $\mathrm{Im}(\gamma) > -\tau_1$. This implies that $F_+^{(1)}$ is analytic in this region, which corresponds to the upper part of the complex plane. Similarly if $f^{(1)}(x)$ has exponential decay given by $\exp(\tau_0 x)$ as x tends to large negative values, then the integral for $F_-^{(1)}$ converges in the lower half plane where $\mathrm{Im}(\gamma) < \tau_0$. Equation (A.1) is only valid in the region where the Fourier transforms given by equation (A.2) converge which is defined by the strip

$$-\tau_1 < \mathrm{Im}(\gamma) < \tau_0.$$

This is referred to as the strip of analyticity. This is also important when we consider the right-hand side of equation (A.1) because the Fourier transform of the kernel function given by j is defined using the infinite series in equation (13) and this does not converge whenever $\sigma + \gamma d \pm \zeta h = 2\pi m$, where m is an integer. We need to specify a strip of analyticity for this function and to achieve this we allow the frequency ω to have a small positive imaginary part. From the definition of ζ given by equation (11), we see that the solutions to $\sigma + \gamma d \pm \zeta h = 2\pi m$ will not lie on the real axis when ω is imaginary and so we obtain a small but finite strip of analyticity where equation (A.1) is valid. Strictly the boundaries for the strip defined by the function j must exceed the limits set by the functions F_+ and F_-. Morse and Feshbach [21, p. 964]. The implications of these conditions is that the solution for D which is obtained using equation (A.1) will only be analytic in the region where $\mathrm{Im}(\gamma) > -\tau_1$ and so the inversion integral for the transform given by equation (9) will be

$$\Delta\phi^{(1)}(x) = \int_{-\infty - \mathrm{i}\tau_1}^{\infty - \mathrm{i}\tau_1} D^{(1)}(\gamma) \mathrm{e}^{-\mathrm{i}\gamma x} \, \mathrm{d}\gamma. \tag{A.3}$$

To solve equation (A.1) we make use of the fact that $F_-^{(1)}$ is only analytic in the lower half plane, while $D^{(1)}$ and $F_+^{(1)}$ are only analytic in the upper half plane. The objective is to split the equation into those parts which are analytic in different regions to establish two equations for the two unknowns $D^{(1)}$ and $F^{(1)}$. To achieve this we factorize the function j as $j = J + J_-$, where the subscripts $+$ or $-$ represent functions which are regular (i.e., have no poles or zeros) in the upper or lower half planes respectively. We then divide through by J_- so that

$$\frac{F_+^{(1)}(\gamma)}{J_-(\gamma)} + \frac{F_-^{(1)}(\gamma)}{J_-(\gamma)} = 2\pi D^{(1)}(\gamma) J_+(\gamma).$$

Since both $F_+^{(1)}$ and J_- are known we split $F_+^{(1)}/J_-$ as

$$F_+^{(1)}(\gamma)/J_-(\gamma) = q_+(\gamma) + q_-(\gamma) \tag{A.4}$$

so that

$$q_-(\gamma) + F_-^{(1)}(\gamma)/J_-(\gamma) = 2\pi D^{(1)}(\gamma) J_+(\gamma) - q_+(\gamma). \tag{A.5}$$

The right-hand side of this equation is analytic in the upper half plane while the left-hand side is analytic in the lower half plane. A consequence of this is that each side of the equation must be equal to an entire function which has no poles in either the upper or the lower half planes and has no influence on the resulting Fourier transforms. This may be taken as equal to zero and so each side of equation (A.5) can be solved independently, giving

$$D^{(1)}(\gamma) = \frac{q_+(\gamma)}{2\pi J_+(\gamma)}. \tag{A.6}$$

The solution therefore depends on finding q_+ and J_+. First consider q_+ for the case given by the boundary condition (19). If γ_0 has a small imaginary part such that $\mathrm{Im}(\gamma_0) - \tau_1 > 0$, we can find $F_+^{(1)}$ by evaluation the integral

$$F_+^{(1)}(\gamma) = \frac{-1}{2\pi} \int_0^\infty w_0 e^{i(\gamma+\gamma_0)x}\, dx = \frac{w_0}{2\pi i(\gamma+\gamma_0)}. \tag{A.7}$$

The assumption that γ_0 has a small imaginary part is required to ensure that the integrand in equation (A.7) tends to zero at large values of x. This implies that the amplitude of the incoming wave tends to zero at large distances downstream from the leading edge. For downstream propagating waves which decay as they propagate this assumption is physically realistic, but for upstream propagating waves this condition implies that they grow in amplitude as they propagate. To circumvent this problem for upstream propagating waves we allow γ_0 to have a small negative imaginary part but specify the strip of analyticity to lie above the real axis so $-\tau_1 - \mathrm{Im}(\gamma_0) > 0$.

To carry out the splitting of the functions required in equation (A.4) we use equation (A.7) to define

$$\frac{F_+^{(1)}(\gamma)}{J_-(\gamma)} = \frac{w_0}{2\pi i(\gamma_0+\gamma)J_-(\gamma)}$$

and split this into two functions as

$$q_+(\gamma) = \frac{w_0}{2\pi i(\gamma_0+\gamma)J_-(-\gamma_0)}, \quad q_-(\gamma) = \frac{w_0}{2\pi i(\gamma_0+\gamma)}\left[\frac{1}{J_-(\gamma)} - \frac{1}{J_-(-\gamma_0)}\right]. \tag{A.8}$$

Hence the pole at $\gamma = -\gamma_0$ is eliminated for q_- and is the only singularity associated with q_+. The consequence of this choice is that we can evaluate $D^{(1)}$ as

$$D^{(1)}(\gamma) = \frac{-iw_0}{(2\pi)^2(\gamma+\gamma_0)J_+(\gamma)J_-(-\gamma_0)} \tag{A.9}$$

and then evaluate the solution of $\Delta\phi^{(1)}(x)$ by inverse transformation as

$$\Delta\phi^{(1)}(x) = \frac{-\mathrm{i}w_0}{(2\pi)^2}\int_{-\infty-\mathrm{i}\tau_1}^{\infty-\mathrm{i}\tau_1} \frac{\mathrm{e}^{-\mathrm{i}\gamma x}}{(\gamma+\gamma_0)J_+(\gamma)J_-(-\gamma_0)}\,\mathrm{d}\gamma. \tag{A.10}$$

We have therefore obtained a complete solution for the discontinuity in potential for a cascade with semi-infinite chord blades. The main difficulty in finding the solution to this equation is in the kernel function so that we can specify the component J_-, and this will be dealt with in the next section. However, first note some of the properties of the result given by equation (A.10). The integral can be evaluated by a contour integration in the complex plane. The integrand is a regular function in the upper half plane and so the value of the integral is zero for $x < 0$. For $x > 0$ the integral is evaluated in the lower half plane where there is a pole at $\gamma = -\gamma_0$ and this corresponds to a wave which propagates along the surface with the incoming wave. In addition, the integrand will have poles at the zeroes of J_+ and contributions from branch lines drawn about the branch points of J_+. To explore the consequence of these zeros and branch lines we need to evaluate the functions $J_\pm$, and this will be carried out in the next section.

A.2. THE SPLITTING OF THE KERNEL FUNCTION

The kernel function is defined in equation (13) by an infinite series and may be summed by using the result that

$$\sum_{n=0}^{\infty} z^n = \frac{1}{1-z}, \quad |z| < 1.$$

The condition that $|z| < 1$ is satisfied when $\mathrm{Im}(\pm\sigma \pm \gamma d + \zeta h) > 0$ which will be the case in the strip of analyticity and so we may write

$$\begin{aligned} j(\gamma) &= \frac{\mathrm{i}\zeta}{4\pi}\sum_{n=-\infty}^{\infty} \mathrm{e}^{\mathrm{i}\gamma nd + \mathrm{i}\zeta|nh| + \mathrm{i}n\sigma} \\ &= \frac{\mathrm{i}\zeta}{4\pi}\left\{\sum_{n=0}^{\infty}\mathrm{e}^{-\mathrm{i}\gamma nd + \mathrm{i}\zeta nh - \mathrm{i}n\sigma} + \sum_{n=0}^{\infty}\mathrm{e}^{\mathrm{i}\gamma nd + \mathrm{i}\zeta nh + \mathrm{i}n\sigma} - 1\right\} \\ &= \frac{\mathrm{i}\zeta}{4\pi}\left\{\frac{1}{1-\mathrm{e}^{-\mathrm{i}\gamma d + \mathrm{i}\zeta h - \mathrm{i}\sigma}} + \frac{1}{1-\mathrm{e}^{\mathrm{i}\gamma d + \mathrm{i}\zeta h + \mathrm{i}\sigma}} - 1\right\}. \end{aligned} \tag{A.11}$$

If we introduce the new variables

$$\begin{aligned} &M = U/c_0, \quad \beta^2 = 1 - M^2, \quad \kappa = \omega/c_0\beta^2, \quad \kappa_e^2 = \kappa^2 - (v/\beta)^2, \\ &\xi = \gamma - \kappa M, \quad \rho = \sigma + \kappa M d, \end{aligned} \tag{A.12}$$

we can write equation (A.11) as

$$j(\gamma) = \frac{\zeta}{4\pi}\left\{\frac{\sin(\zeta h)}{\cos(\zeta h) - \cos(\xi d + \rho)}\right\}, \quad \zeta = \beta\sqrt{\kappa_e^2 - \xi^2}. \tag{A.13}$$

To obtain the split function $J_{\pm}(\gamma)$, we first consider the function $\zeta \sin \zeta h$, which can be expanded as an infinite product (see Morse and Feshbach [21 (p. 385)]. The expansion is

$$\zeta \sin \zeta h = \kappa_e \beta \sin(\kappa_e h\beta) \prod_{m=0}^{\infty} (1 - \xi/\theta_m)(1 - \xi/\vartheta_m), \tag{A.14}$$

where

$$\theta_m = -\sqrt{\kappa_e^2 - (m\pi/\beta h)^2}, \qquad \vartheta_m = \sqrt{\kappa_e^2 - (m\pi/\beta h)^2} \tag{A.15}$$

are the zeros of the function. The first term in the infinite product has zeros in the lower half plane and the second term has zeros in the upper half plane.

The denominator of j may be expanded in a similar fashion giving

$$\cos(\zeta h) - \cos(\xi d + \rho) = [\cos(\kappa_e h\beta) - \cos(\rho)] \prod_{m=-\infty}^{\infty} (1 - \xi/\eta_m^+)(1 - \xi/\eta_m^-)e^{C\xi}, \tag{A.16}$$

where C is a constant which will be eliminated later and $\eta_m^{\pm}$ are the zeros of the function defined as

$$\eta_m^{\pm} = -f_m \sin \chi_e \pm \cos \chi_e \sqrt{\kappa_e^2 - f_m^2}, \quad f_m = \frac{\sigma + \kappa M d - 2\pi m}{\sqrt{d^2 + (h\beta)^2}} \tag{A.17}$$

and $\tan \chi_e = d/h\beta$.

These expansions clearly define the zeros and poles of the function j and so to obtain the factorization we can separate out two sets of functions which only have zeros or poles in either the upper or the lower half planes. This gives the factorization as

$$J_+(\gamma) = \frac{\kappa_e \beta \sin(\kappa_e h\beta)}{4\pi(\cos(\kappa_e h\beta) - \cos(\rho))} \frac{\prod_{m=0}^{\infty}(1 - \xi/\theta_m)}{\prod_{m=-\infty}^{\infty}(1 - \xi/\eta_m^-)} e^{\Phi},$$

$$J_-(\gamma) = \frac{\prod_{m=0}^{\infty}(1 - \xi/\vartheta_m)}{\prod_{m-\infty}^{\infty}(1 - \xi/\eta_m^+)} e^{-\Phi}. \tag{A.18}$$

The function Φ must be chosen so that both J_+ and J_- have algebraic growth as ξ tends to infinity and is given by

$$\Phi = \frac{-\mathrm{i}\xi}{\pi}\{h\beta \log(2\cos\chi_e) + \chi_e d\}. \tag{A.19}$$

A.3. THE FIRST ORDER CORRECTION FOR THE EFFECT OF FINITE CHORD

In section A.1 we obtained a solution for the cascade with infinite chord. We now make a first order correction to this solution to account for the finite chord of the blade by applying the boundary conditions specified in equation (16) and obtaining a solution to equation (19) with $i = 2$. We follow the same procedure as in section A.1 starting with the Fourier transform of equation (19) which in this case can be written as

$$F_+^{(2)}(\gamma) = 2\pi[D_-^{(2)}(\gamma) + D_+^{(2)}(\gamma)]j(\gamma), \tag{A.20}$$

where we have used the Fourier transforms

$$F_+^{(2)}(\gamma) = \frac{1}{2\pi}\int_c^\infty f^{(2)}(x)\mathrm{e}^{\mathrm{i}\gamma x}\,\mathrm{d}x, \quad D_+^{(2)}(\gamma) = \frac{1}{2\pi}\int_c^\infty \Delta\phi_0^{(2)}(x)\mathrm{e}^{\mathrm{i}\gamma x}\,\mathrm{d}x,$$

$$D_-^{(2)}(\gamma) = \frac{1}{2\pi}\int_{-\infty}^c \Delta\phi_0^{(2)}(x)\mathrm{e}^{\mathrm{i}\gamma x}\,\mathrm{d}x. \tag{A.21}$$

The unknowns in this problem are $F_+^{(2)}$ and $D_-^{(2)}$ and we can specify $D_+^{(2)}$ using the boundary condition given by equation (21). Using the properties of Fourier transforms this gives

$$-\mathrm{i}(\omega + \gamma U)D_+^{(2)}(\gamma)\mathrm{e}^{-\mathrm{i}\omega' t + \mathrm{i}vz} = \frac{-1}{2\pi}\int_c^\infty \frac{\mathrm{D}}{\mathrm{D}t}(\Delta\phi_0^{(1)}(x)\mathrm{e}^{-\mathrm{i}\omega' t + \mathrm{i}vz})\mathrm{e}^{\mathrm{i}\gamma x}\,\mathrm{d}x. \tag{A.22}$$

The integral can be evaluated by substituting from the inversion integral equation (A.10) to give

$$-\mathrm{i}(\omega + \gamma U)D_+^{(2)}(\gamma) = \frac{-1}{2\pi}\int_c^\infty \frac{-\mathrm{i}w_0}{(2\pi)^2}\int_{-\infty-\mathrm{i}\tau_1}^{\infty-\mathrm{i}\tau_1} \frac{-\mathrm{i}(\omega+\gamma_1 U)\mathrm{e}^{-\mathrm{i}(\gamma_1-\gamma)x}}{(\gamma_1+\gamma_0)J_+(\gamma_1)J_-(-\gamma_0)}\,\mathrm{d}\gamma_1\,\mathrm{d}x. \tag{A.23}$$

In the strip of analyticity we require that $\mathrm{Im}(\gamma) > -\tau_1$ and so $\mathrm{Im}(\gamma - \gamma_1) > \mathrm{Im}(\gamma - \tau_1) > 0$ and we can carry out the integral over x to obtain

$$-\mathrm{i}(\omega + \gamma U)D_+^{(2)}(\gamma) = \frac{w_0}{(2\pi)^3}\int_{-\infty - \mathrm{i}\tau_1}^{\infty - \mathrm{i}\tau_1} \frac{(\omega + \gamma_1 U)\mathrm{e}^{-\mathrm{i}(\gamma_1 - \gamma)c}}{\mathrm{i}(\gamma_1 - \gamma)(\gamma_1 + \gamma_0)J_+(\gamma_1)J_-(-\gamma_0)}\mathrm{d}\gamma_1. \tag{A.24}$$

This integral may be evaluated by using a contour in the lower half plane which encloses the poles at $\gamma_1 = -\gamma_0$ and at the zeros of J_+. We can write the solution in the form

$$-\mathrm{i}(\omega + \gamma U)D_+^{(2)}(\gamma) = \sum_n \frac{A_n \mathrm{e}^{\mathrm{i}(\gamma - \delta_n)c}}{\gamma - \delta_n}, \tag{A.25}$$

where A_n are the residues of the poles which lie at δ_n and can be calculated as

$$A_0 = \frac{w_0(\omega - \gamma_0 U)}{(2\pi)^2 j(-\gamma_0)}, \quad \delta_0 = -\gamma_0,$$

$$A_n = \frac{w_0(\omega + \delta_n U)}{(2\pi)^2(\delta_n + \gamma_0)J'_+(\delta_n)J_-(-\gamma_0)}, \quad \delta_n = \kappa M + \theta_{n-1}, \quad n > 0, \tag{A.26}$$

with θ_n defined by equation (A.15). To obtain J'_+ we note that

$$\left[\frac{\partial J_+}{\partial \gamma}\right]_{\gamma = \delta_n} = \left[\frac{\partial (j/J_-)}{\partial \gamma}\right]_{\gamma = \delta_n} = \left[\frac{j'}{J'} - \frac{jJ'_-}{J_-^2}\right]_{\gamma = \delta_n} = \frac{j'(\delta_n)}{J_-(\delta_n)},$$

where j' is relatively easy to evaluate as

$$j'(\delta_n) = \frac{(\kappa M - \delta_n)h\beta^2}{4\pi(1 - \cos(\delta_n d + \sigma)\cos((n-1)\pi))} \begin{cases} 2, & n = 1, \\ 1, & n > 1, \end{cases} \tag{A.27}$$

We next substitute equation (A.25) into equation (A.20) and split the function j so that

$$\frac{-\mathrm{i}(\omega + \gamma U)F_+^{(2)}(\gamma)}{2\pi J_+(\gamma)} = \left\{\sum_{n=0}^{\infty} \frac{A_n \mathrm{e}^{\mathrm{i}(\gamma - \delta_n)c}}{\gamma - \delta_n}\right\} J_-(\gamma) - \mathrm{i}(\omega + \gamma U)D_-^{(2)}(\gamma)J_-(\gamma). \tag{A.28}$$

We can then rearrange this equation to ensure that the left-hand side is analytic in the upper half plane while the right-hand side is analytic in the lower half plane.

This is achieved by eliminating the poles from the terms in brackets to give

$$\frac{-\mathrm{i}(\omega+\gamma U)F_+^{(2)}(\gamma)}{2\pi J_+(\gamma)} - \left\{\sum_{n=0}^{\infty}\frac{A_n \mathrm{e}^{\mathrm{i}(\gamma-\delta_n)c}J_-(\delta_n)}{\gamma-\delta_n}\right\}$$
$$= \left\{\sum_{n=0}^{\infty}\frac{A_n \mathrm{e}^{\mathrm{i}(\gamma-\delta_n)c}(J_-(\gamma)-J_-(\delta_n))}{\gamma-\delta_n}\right\} - \mathrm{i}(\omega+\gamma U)D_-^{(2)}(\gamma)J_-(\gamma). \tag{A.29}$$

We then obtain an expression for the unknown quantities and can define

$$D_-^{(2)}(\gamma) = \left\{\sum_{n=0}^{\infty}\frac{A_n \mathrm{e}^{\mathrm{i}(\gamma-\delta_n)c}(1-J_-(\delta_n)/J_-(\gamma))}{\mathrm{i}(\omega+\gamma U)(\gamma-\delta_n)}\right\}. \tag{A.30}$$

Combining this with equation (A.25) we find a solution for $D^{(2)}$ which is valid in the strip of analyticity and is given by

$$D^{(2)}(\gamma) = \left\{-\sum_{n=0}^{\infty}\frac{A_n \mathrm{e}^{\mathrm{i}(\gamma-\delta_n)c}}{\mathrm{i}(\omega+\gamma U)(\gamma-\delta_n)}\left[\frac{J_-(\delta_n)}{J_-(\gamma)}\right]\right\}. \tag{A.31}$$

This gives the first order correction for the effect of the trailing edge on the cascade response and should be added to the result given by equation (A.9) for the cascade with semi-infinite blade chord. However, the inverse transform of this function should be evaluated from the two separate parts defined for positive and negative values of x.

These results have some important features which are worthy of discussion and provide some insight into the mechanisms associated with this solution. First we note that the coefficient of the $n=0$ term in this series given by equation (A.26) will be zero for a two-dimensional vortical incident gust for which $\gamma_0 = \omega/U$. If this were not the case then $D^{(2)}$ would have a pole of second order at $\gamma = \omega/U$. Next consider the sum of $D^{(1)}$ and $D^{(2)}$ which gives the combined solution. We note that the solution for $D^{(1)}$ given by equation (A.9) has poles at $\gamma = -\gamma_0$ and the zeros of J_+ which correspond to the points $\gamma = \delta_n$. The residue at these poles is

$$\frac{\mathrm{i}w_0}{(2\pi)^2 j(-\gamma_0)} \quad \text{and} \quad \frac{\mathrm{i}w_0}{(2\pi)^2(\delta_n+\gamma_0)J_+'(\delta_n)J_-(-\gamma_0)}$$

and is exactly cancelled by the residues at the same poles in the series defining $D^{(2)}$. The only singularities of the sum $D^{(1)}+D^{(2)}$ occur at $\gamma = -\omega/U$ and at the zeros of J_- in the upper half plane. The pole at $\gamma = -\omega/U$ represents a convected wave which causes a discontinuity in velocity extending downstream in the wake, but this pole does not induce any pressure discontinuity, and it can be shown that it cannot be responsible for radiating any sound. The poles at the zeros of J_- on the other hand are spurious since they only occur in $D_-^{(2)}$ and so are associated with the discontinuity of potential which the solution has induced upstream of the leading edge of the blade. We must therefore introduce additional corrections specified by

the boundary conditions given in equations (22) and (23) to obtain an accurate solution, and this will be the purpose of the next section.

A.4. SECOND ORDER CORRECTIONS FOR THE EFFECTS OF THE LEADING AND TRAILING EDGES

To obtain the second order corrections for the cascade response function, we will first solve the problem specified by the boundary conditions in equation (22) and then consider the problem specified in equation (23). Since these problems are coupled we will not be able to find the complete solution of each independently, and so the solution to the first will not be complete until we have solved the second. First, we specify the Fourier transform of equation (19) which can be written as

$$F_{-}^{(3)}(\gamma) = 2\pi[D_{-}^{(3)}(\gamma) + D_{+}^{(3)}(\gamma)]j(\gamma), \tag{A.32}$$

where we have defined $D_{\pm}^{(3)}$ on the right-hand side using the Fourier transforms

$$D_{+}^{(3)}(\gamma) = \frac{1}{2\pi}\int_{0}^{\infty} \Delta\phi_0^{(3)}(x)\mathrm{e}^{\mathrm{i}\gamma x}\,\mathrm{d}x, \quad D_{-}^{(3)}(\gamma) = \frac{1}{2\pi}\int_{-\infty}^{0} \Delta\phi_0^{(3)}(x)\mathrm{e}^{\mathrm{i}\gamma x}\,\mathrm{d}x. \tag{A.33}$$

The boundary condition (22) can be used to specify $D_{-}^{(3)}$ and, as was done in section A.3, we make use of the inversion integral and the residue theorem to obtain a result. However, note that the upper limit of integration for $D_{-}^{(3)}$ in equation (A.33) is zero and can be replaced by $-\varepsilon$ in the limit that ε is small and positive. Then we obtain

$$D_{-}^{(3)}(\gamma) = \frac{-1}{2\pi}\int_{-\infty}^{-\varepsilon}\int_{-\infty+\mathrm{i}\tau_0}^{\infty+\mathrm{i}\tau_0} [D_{-}^{(2)}(\gamma_1) + D_{-}^{(4)}(\gamma_1)]\mathrm{e}^{-\mathrm{i}(\gamma_1-\gamma)x}\,\mathrm{d}\gamma_1\,\mathrm{d}x. \tag{A.34}$$

In the strip of analyticity we require the $\mathrm{Im}(\gamma) < \tau_0$ and so we can carry out the integral over x to obtain

$$D_{-}^{(3)}(\gamma) = \frac{1}{2\pi}\int_{-\infty+\mathrm{i}\tau_0}^{\infty+\mathrm{i}\tau_0} \frac{[D_{-}^{(2)}(\gamma_1) + D_{-}^{(4)}(\gamma_1)]}{\mathrm{i}(\gamma_1-\gamma)}\mathrm{e}^{\mathrm{i}(\gamma_1-\gamma)\varepsilon}\,\mathrm{d}\gamma_1. \tag{A.35}$$

This integral may be evaluated by closing the contour in the upper half of the complex plane and the result will be given by the sum of the residues of the integrand which lie within this contour. Since we have yet to evaluate $D^{(4)}$, we cannot evaluate the integral at this stage but if it is assumed that the integrand only has simple poles in the upper half plane then we can specify the form of the solution as

$$D_{-}^{(3)}(\gamma) = -\sum_{m}\frac{B_m}{(\gamma-\varepsilon_m)}, \tag{A.36}$$

where B_m is the residue of the poles of the functions in [ ] as defined in equation (A.35), and ε_m are the location of the poles in the complex plane. Placing this result in equation (A.32) and splitting the equation so that the right-hand side is analytic in the lower half plane and the right-hand side is analytic in the upper half plane gives

$$\frac{F_-^{(3)}(\gamma)}{2\pi J_-(\gamma)} + \sum_m \frac{B_m J_+(\varepsilon_m)}{\gamma - \varepsilon_m} = \sum_m \frac{B_m(J_+(\varepsilon_m) - J_+(\gamma))}{\gamma - \varepsilon_m} + D_+^{(3)}(\gamma)J_+(\gamma). \tag{A.37}$$

We then obtain a solution for $D_+^{(3)}$ as

$$D_+^{(3)}(\gamma) = -\sum_m \frac{B_m}{(\gamma - \varepsilon_m)}\left[\frac{J_+(\varepsilon_m)}{J_+(\gamma)} - 1\right]. \tag{A.38}$$

The solution is not complete until the last part of the problem is solved. This is given by the solution to equation (19) subject to the boundary conditions given by equation (23). Note that the specification of this problem is identical to the specification of the trailing-edge correction given by equation (21), and this is expected since the purpose of this correction is to ensure that the solution given above does not cause a pressure discontinuity downstream of the trailing edge. To obtain the solution for the boundary conditions given by equation (23), we specify the Fourier transform of equation (19) in exactly the same form as equation (A.20) with the superscript (2) changed to (4) and use the transforms defined by equation (A.21). We then evaluate the value of $D_+^{(4)}$ using the integral of the form given in equation (A.22) with the superscript (1) changed to (3) and then evaluate this integral as in equation (A.23) to obtain

$$-\mathrm{i}(\omega + \gamma U)D_+^{(4)}(\gamma) = \frac{1}{2\pi}\int_c^\infty \int_{-\infty - \mathrm{i}\tau_1}^{\infty - \mathrm{i}\tau_1} \mathrm{i}(\omega + \gamma_1 U)D_+^{(3)}(\gamma_1)\mathrm{e}^{-\mathrm{i}(\gamma_1 - \gamma)x}\,\mathrm{d}\gamma_1\,\mathrm{d}x. \tag{A.39}$$

Evaluating the integral over x and substituting equation (A.38) then gives

$$-\mathrm{i}(\omega + \gamma U)D_+^{(4)}(\gamma) = \frac{-1}{2\pi}\int_{-\infty - \mathrm{i}\tau_1}^{\infty - \mathrm{i}\tau_1} \sum_m \frac{(\omega + \gamma_1 U)B_m}{(\gamma_1 - \gamma)(\gamma_1 - \varepsilon_m)}\left[\frac{J_+(\varepsilon_m)}{J_+(\gamma_1)} - 1\right]\mathrm{e}^{-\mathrm{i}(\gamma_1 - \gamma)c}\,\mathrm{d}\gamma_1. \tag{A.40}$$

This integral may be evaluated by using a contour in the lower half plane which encloses all the poles in the integrand. These poles occur at the zeros of J_+ and this leads to the solution for $D_+^{(4)}$ which is in the same form as equation (A.25) and is given by

$$-\mathrm{i}(\omega + \gamma U)D_+^{(4)}(\gamma) = \sum_{n=0}^{\infty} \frac{C_n \mathrm{e}^{\mathrm{i}(\gamma - \delta_n)c}}{\gamma - \delta_n}, \tag{A.41}$$

where the coefficients C_n are given by

$$C_0 = 0, \quad C_n = \sum_m \frac{\mathrm{i}(\omega + \delta_n U)}{(\varepsilon_m - \delta_n)} \left[\frac{J_+(\varepsilon_m)}{J'_+(\delta_n)} \right] B_m, \quad n > 0. \tag{A.42}$$

Finally, we obtain the solution for $D^{(4)}_{-}$ in the same form as equation (A.30):

$$D^{(4)}_{-}(\gamma) = \left\{ \sum_{n=0}^{\infty} \frac{C_n \mathrm{e}^{\mathrm{i}(\gamma - \delta_n)c}(1 - J_-(\delta_n)/J_-(\gamma))}{\mathrm{i}(\omega + \gamma U)(\gamma - \delta_n)} \right\}. \tag{A.43}$$

Combining this with equation (A.41) we find a solution for $D^{(4)}$ which is valid in the strip of analyticity and is given by

$$D^{(4)}(\gamma) = \left\{ \sum_{n=0}^{\infty} \frac{\mathrm{i}C_n \mathrm{e}^{\mathrm{i}(\gamma - \delta_n)c} J_-(\delta_n)}{(\omega + \gamma U)(\gamma - \delta_n) J_-(\gamma)} \right\}. \tag{A.44}$$

However, we still need to define the coefficients B_m which are the residues of the poles of the function $D^{(2)}_{-} + D^{(4)}_{-}$ in the upper half plane. Using equations (A.30) and (A.43) we obtain

$$D^{(2)}_{-}(\gamma) + D^{(4)}_{-}(\gamma) = \left\{ \sum_{n=0}^{\infty} \frac{(A_n + C_n)\mathrm{e}^{\mathrm{i}(\gamma - \delta_n)c}(1 - J_-(\delta_n)/J_-(\gamma))}{\mathrm{i}(\omega + \gamma U)(\gamma - \delta_n)} \right\}, \tag{A.45}$$

which has simple poles at the zeros of J_-, which proves our earlier assumption and allows us to define

$$B_m = -\sum_{n=0}^{\infty} \frac{(A_n + C_n)\mathrm{e}^{\mathrm{i}(\varepsilon_m - \delta_n)c}}{\mathrm{i}(\omega + \varepsilon_m U)(\varepsilon_m - \delta_n)} \left[\frac{J_+(\delta_n)}{J'_-(\varepsilon_m)} \right], \tag{A.46}$$

where ε_m are the zeros of J_- which may be obtained from equation (A.15) since $\varepsilon_m = \kappa M + \vartheta_{m-1}$ $(m > 0)$. We now have a pair of equations which relate the coefficients B_m and C_m. Unfortunately, these are defined in terms of infinite series and so cannot be solved exactly. However, if the series are truncated after a finite number of terms then solutions can be obtained. To this end we write the truncated series in matrix form as

$$[\mathbf{F}_{mn}]\{\{A_n\} + \{C_n\}\} + A_0 G_m = \{B_m\}, \quad [\mathbf{L}_{mn}]\{B_n\} = \{C_m\}, \quad n, m > 0, \tag{A.47}$$

where the coefficients are defined as

$$F_{mn} = -\frac{e^{i(\varepsilon_m - \delta_n)c}}{i(\omega + \varepsilon_m U)(\varepsilon_m - \delta_n)}\left[\frac{J_-(\delta_n)}{J'_-(\varepsilon_m)}\right], \quad G_m = -\frac{e^{i(\varepsilon_m - \delta_0)c}}{i(\omega + \varepsilon_m U)(\varepsilon_m - \delta_0)}\left[\frac{J_-(\delta_0)}{J'_-(\varepsilon_m)}\right], \tag{A.48}$$

$$L_{mn} = \frac{i(\omega + \delta_m U)}{(\varepsilon_n - \delta_m)}\left[\frac{J_+(\varepsilon_n)}{J'_+(\delta_n)}\right]. \tag{A.49}$$

we obtain

$$\{B_m\} = [[\mathbf{1}] - [\mathbf{F}_{mn}][\mathbf{L}_{mn}]]^{-1}\{\{\mathbf{F}_{mn}\}\{A_n\} + A_0 G_m\} \tag{A.50}$$

and we have the complete solution for all the coefficients.

Adding together all the solutions we obtain the Fourier transform of the discontinuity in velocity potential as

$$D(\gamma) = \frac{iw_0}{(2\pi)^2(\gamma + \gamma_0)J_+(\gamma)J_-(-\gamma_0)}$$
$$-\left\{\sum_{n=0}^{\infty}\frac{(A_n + C_n)e^{i(\gamma - \delta_n)c}}{i(\omega + \gamma U)(\gamma - \delta_n)}\left[\frac{J_-(\delta_n)}{J_-(\gamma)}\right]\right\} - \left\{\sum_{n=0}^{\infty}\frac{B_m}{(\gamma - \varepsilon_m)}\left[\frac{J_+(\varepsilon_m)}{J_+(\gamma)}\right]\right\}. \tag{24}$$